PROC. 19th INT. CONF. HIGH ENERGY PHYSICS
TOKYO, 1978

P 1b Hadron–Hadron Reactions, High Multiplicity

R. DIEBOLD

Argonne National Laboratory, Argonne, Illinois 60439

§1. Introduction

This talk covers results presented in four parallel sessions:

	Contributed Papers
A3 —High Energy Hadron Reactions, High Multiplicity	75
B7 —Charm Searches and Related Topics	29
B10—Ultrahigh Energy Events and Exotic Phenomena (Cosmic Rays)	18
B11—Nuclear Effects in High Energy Collisions and Related Topics	58
	180

It thus has a broader range of topics than the title would suggest. As can be seen by the number of contributed papers, these fields are quite active; in particular, many results were contributed on high multiplicity or inclusive type studies and on reactions taking place off nuclei.

Although these topics have generally been studied for several years now, many of the contributions add valuable data at new energies or for different beam particles, and are useful in making compilations and detailed fits to the data. Such a multitude of numerical results is, however, somewhat difficult to cover adequately in a rapporteur talk. Fortunately, many of these subjects were covered in detail by the mini-rapporteurs in the parallel sessions. In any case, with 180 papers, roughly 16% of the total contributed to the Conference, I cannot possibly cover all the results and I apologize to those whose hard work has not been adequately covered.

§2. Two and Three Body Correlations

Kenney *et al.* (paper 496) have looked at π^-p reactions at several energies in bubble chambers, including 30,000 events at 360 GeV/c. They have analyzed the dependence of the two-body correlation function

$$R=\frac{\rho_2(y_1, y_2)}{\rho_1(y_1)\rho_1(y_2)}-1, \tag{1}$$

$$\rho_1(y)=\frac{1}{\sigma}\frac{\mathrm{d}\sigma}{\mathrm{d}y}, \tag{2}$$

$$\rho_2(y_1, y_2)=\frac{1}{\sigma}\frac{\mathrm{d}^2\sigma}{\mathrm{d}y_1\mathrm{d}y_2}, \tag{3}$$

on multiplicity and incident momentum.

The 360-GeV/c data are combined with results at 18.5, 100, and 200 GeV/c to evaluate cluster parameters. Some of the two-body correlations for unlike charged particles near $y_1=y_2=0$ are shown in Fig. 1, both as a function of multiplicity and as a function of energy. Note that the authors use only ≥ 8 prongs in order to avoid diffractive effects. In the Berger cluster model[1]

$$R_n^{+-}(0, 0)=\frac{\langle k\rangle^{+-}}{n}\left[\frac{\ln s}{2\sqrt{\pi}\delta}-1\right] \tag{4}$$

where $\langle k\rangle^{+-}$ is the numbers of charged particles per cluster and δ is the correlation length, $\langle y_2-y_1\rangle_{\mathrm{rms}}$. When plotted using the scales shown in Fig. 1, the model expects straight lines, as observed. Note that unlike most experiments, with results at only one energy, these authors can use the various energies to give a consistency check on the method. After checking the consistency, they simultaneously fit the dependence on multiplicity and energy and find that on average there are 1.60 ± 0.12 charged particles per cluster and $\delta=0.99\pm0.03$.

With the present high statistics available from bubble chamber experiments the same set of authors (paper 497) were able to observe three-body dynamical correlations. For this purpose they use the definition

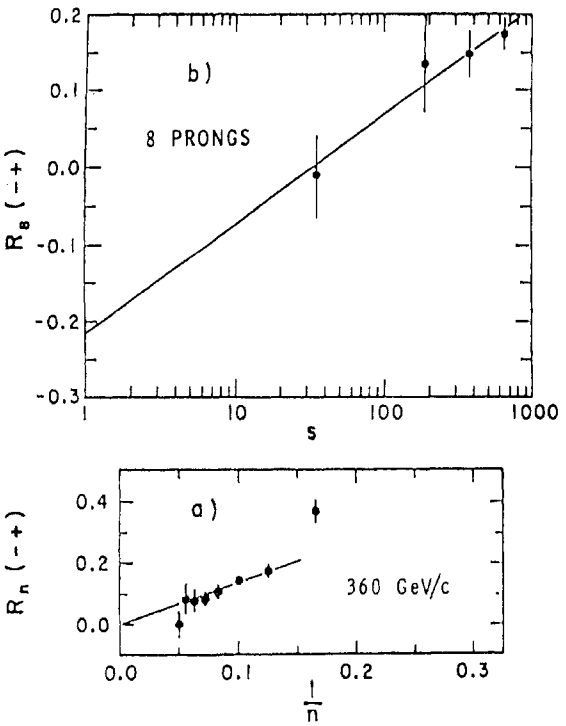

Fig. 1. Energy and multiplicity depencence of the two body correlation functions for unlike-charge pairs produced in π^-p reactions at $y_1=y_2=0$ (Kenney *et al.* paper 496).

$$R_3=\frac{(123)-(12)(3)-(23)(1)-(31)(2)+2(1)(2)(3)}{(1)(2)(3)}, \tag{5}$$

where

$$(123)\equiv\rho_3(y_1, y_2, y_3)=\frac{1}{\sigma}\frac{\mathrm{d}^3\sigma}{\mathrm{d}y_1\mathrm{d}y_2\mathrm{d}y_3}, \text{ etc.} \tag{6}$$

Note that the effects coming from two-body correlations are explicitly removed. Figure 2 shows the results, both for all three particles having negative charge and for the $-+-$combination. As expected, they do not observe any correlation between three negatively charged particles. They do, however, see a significant effect near $y_1=y_2=y_3=0$ for the $-+-$ combination; this effect is apparently narrower than the two-body correlations, with a width of perhaps $\pm 1/2$ unit of rapidity. The three-body correlation observed is considerably smaller than found for the two body case:

$R_2(0, 0)$		$R_3(0, 0, 0)$	
$+-$	0.69 ± 0.05	$-+-$	0.26 ± 0.07
$--$	0.23 ± 0.07	$---$	0.01 ± 0.06

A smaller three-body correlation would, of course, be expected if the average cluster does

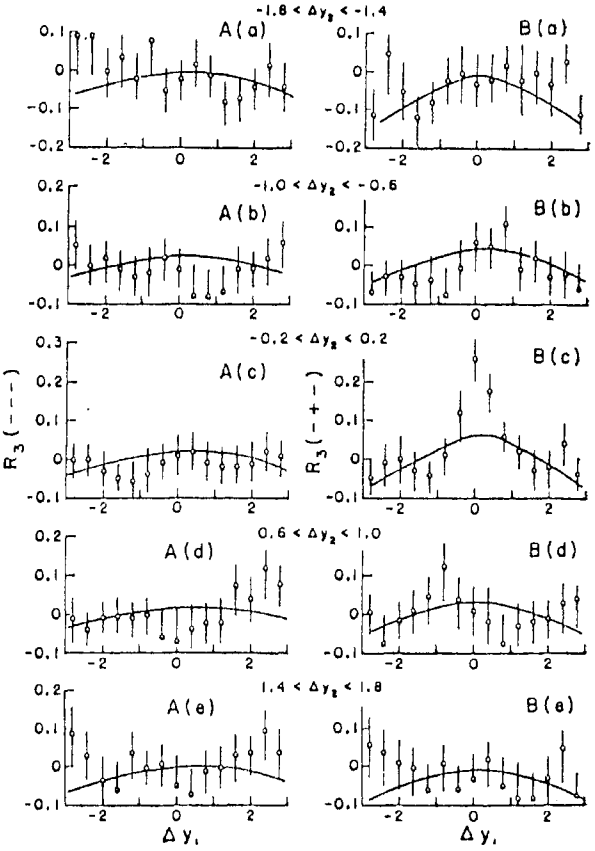

Fig. 2. Dynamical three-body correlation for π^-p reactions at 200 GeV/c as a function of $\Delta y_1=y_1=y_2$ for various intervals of $\Delta y_2=y_2-y_3$. Values for the $(---)$ charge combination are shown on the left, and for the $(-+-)$ on the right. The smooth curves are from a Monte Carlo simulation which includes no explicit short-range correlations (Kenney *et al.* paper 497).

indeed have only 1.6 charged particles.

We next consider the results of a high statistics ISR experiment carried out in the split field magnet at $\sqrt{s}=52$ GeV by the CCHK collaboration (Drijard *et al.* paper 273). To avoid diffractive effects they cut on -7 reconstructed tracks, leaving a sample of $\sim$200,000 events. Figure 3 shows the two-body correlation function, with positive correlations for $y_2=0$ and 2, but a negative correlation out near the kinematic limit, $y_2=-4$. Qualitatively this effect is well fit by various cluster models, the results of the independent emission of charged clusters being shown in the figure. They find a correlation length very similar to that of the previous experiment, an average of 1.8 charged particles per cluster, and one cluster per unit rapidity.

Figure 4 shows the change in charge density at y_1 when the trigger particle at y_2 of negative

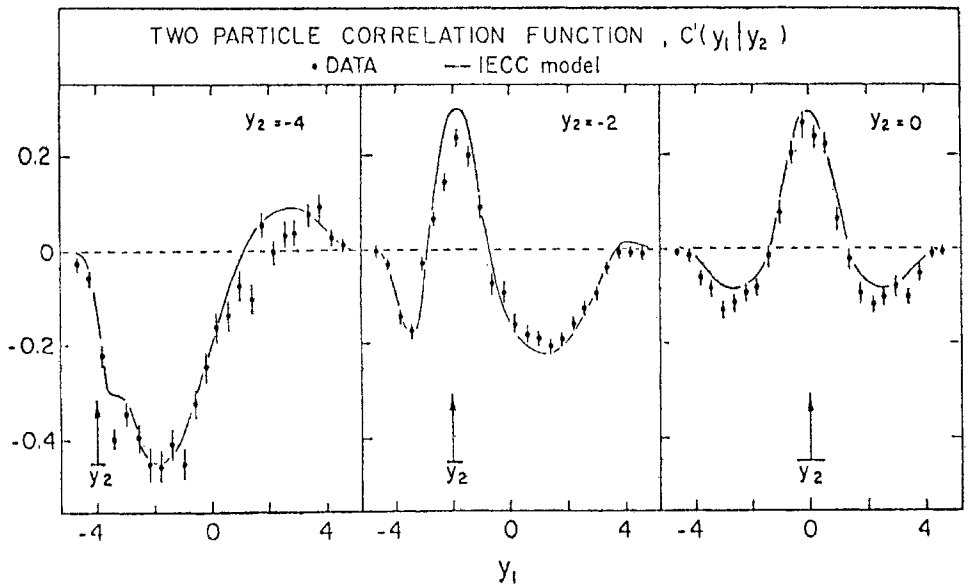

Fig. 3. Two body correlation function in non-diffractive ($n_{obs} \geq 7$) pp collisions at $\sqrt{s} = 52.5$ GeV for different values of y_2. The lines are the predictions of a cluster model with independent emission of charged clusters (Drijard *et al.* paper 273).

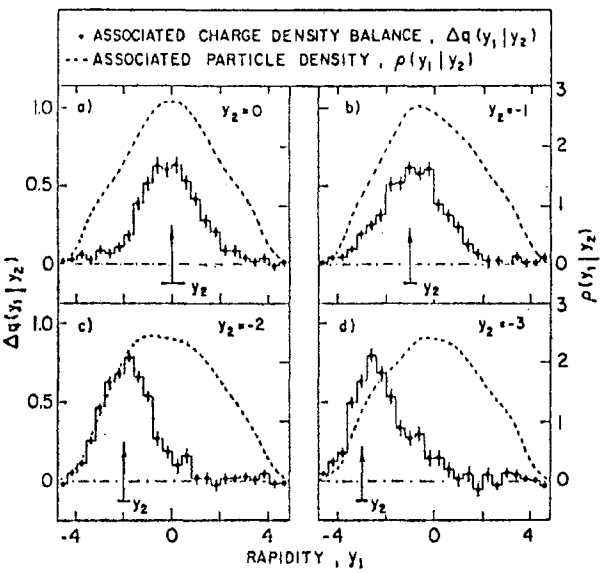

Fig. 4. Associated charge density balance (Drijard *et al.* paper 273).

charge is replaced by one of positive charge. The data show a local compensation of charge, much narrower than the associated particle density distribution; this allows a partial discrimination between the various models considered by these authors.

They have also looked at the distribution of transverse momentum compensation, and find that unlike charge compensation, p_T is compensated globally in agreement with both their uncorrelated jet model and correlated cluster link model. The authors tend to favor the latter model which can be used to obtain[2]

$$\alpha'_P(0) = 0.26/\text{GeV}^2 \qquad (7)$$

for the slope of the Pomeron trajectory. They also obtain an average mass for the clusters of 1.3 GeV, with an average transverse momentum of (0.65 ± 0.10) GeV/c, comparable to that observed for meson resonances in this mass region.[3]

Other methods have also been used to define clusters in attempts to understand multi-particle reactions. Pless *et al.* (paper 551) use charge distributions to define zones; they find that most of the multi-particle events can be described as having two leading particles or clusters, plus a central isotropically decaying fireball. An alternate method finds clusters of charged particles using a nearest neighbor technique.[4] This latter technique yields a p_T distribution for clusters of charged particles which matches on rather well to the jet cross sections found by Bromberg *et al.*[5] at larger p_T.

§3. Second Order (Bose–Einstein) Interference

A few years ago Kopylov, Podgoretsky and Cocconi[6] suggested the use of like-particle (*e.g.*, $\pi^-\pi^-$) correlations to estimate the dimensions and lifetime of emission (not interaction) regions. This is similar to a method used over the past 20 years by radioastronomers and has been used in other fields as well.

In principle, this technique is of particular interest because one can examine the emis-

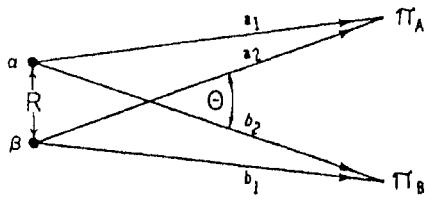

Fig. 5. Sketch showing two identical pions combing from two sources; used to derive eq. 8.

sion regions for the various classes of events such as high $-p_T$ events, events having $\bar{p}$'s, or as a function of multiplicity.

For example, consider the two π^-'s (π_A and π_B) coming from points α and β in Fig. 5. Since we can't tell which source gave which π, we must add the amplitudes:

$$|\mathrm{Amp}|^2=|\underbrace{e^{ika_1}e^{ikb_1}}_{\substack{\alpha\to A\\ \beta\to B}}+\underbrace{e^{ika_2}e^{ikb_2}}_{\substack{\alpha\to B\\ \beta\to A}}|^2=2(1+\cos Rk\theta) \tag{8}$$

Integrating these points over a sphere yields the relation

$$\frac{N_{\pi^\pm\pi^\pm}}{N_{\pi^+\pi^-}}=C\left[1+\lambda\frac{(2J_1(Rq_t)/(Rq_t)^2}{1+(q_0\tau)^2}\right] \tag{9}$$

where

q_t=component of $\boldsymbol{p}_1-\boldsymbol{p}_2$ transverse to $\boldsymbol{p}_1+\boldsymbol{p}_2$

$q_0=E_1-E_2$ (in CM system).

The coefficient λ allows for the fact that not all of the π^- may be able to interfere with one another, and the normalization on the left-hand side neglects possible resonant effects in the low-mass $\pi^+\pi^-$ system.

Three sets of bubble chamber data are shown in Fig. 6 (Deutschmann *et al.*[7]) together with fits to eq. 9. The data are well fit by this form, with the enhancement being largest near $q_t=q_0=0$ as expected. These authors find that the radius of the emission region is independent of the reaction, and also, at least for the high-statistics π^+p data, independent of multiplicity, $R=(1.85\pm0.15)$f. They also find the lifetime parameter to be $c\tau=(1.2\pm 0.3)$f. The interference is strongest for the $p\bar{p}$ case with λ close to unity, while it is only half this value for the higher energy π^+ and K^- beams.

These values are compared with results from other experiments[8] in Fig. 7, which includes several new results presented to this Conference. While there is considerable spread in the results from the different experiments, the radii of Deutschmann *et al.* appear larger than found in most of the previous experiments. They have reanalyzed some of the previous data, in particular allowing λ to vary

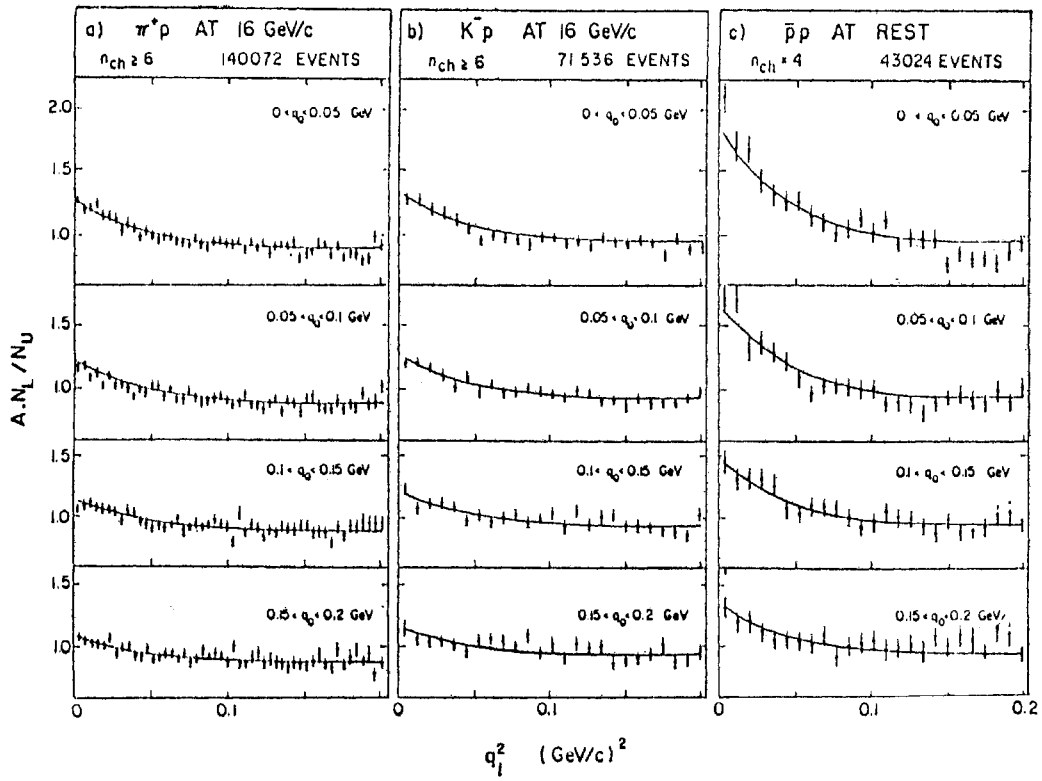

Fig. 6. Normalized ratio of the numbers of pion pairs of like and unlike charges, fit to eq. 9. From ref. 7.

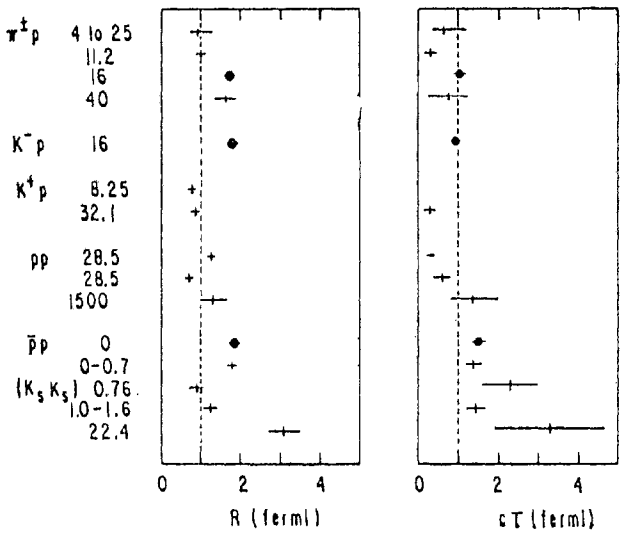

Fig. 7. Compilation of results on the source parameters obtained from Bose-Einstein interference fits. The circles are from Deutschmann *et al.* (ref. 7); see ref. 8 for the other points.

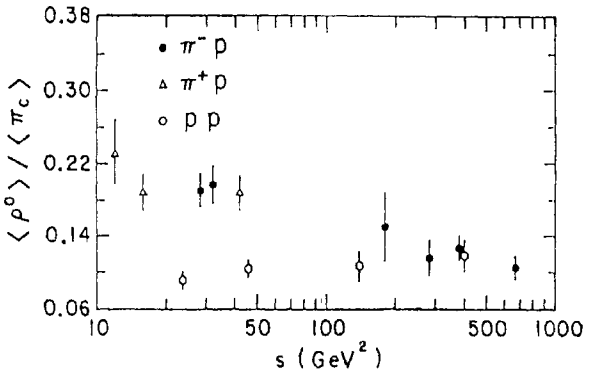

Fig. 8. Compilation of the average number of ρ^0's per produced pion pair as a function of energy for $\pi^{\pm}$p and pp interactions (Kenney *et al.* paper 500).

rather than fixing it to unity, and find results closer to their own than to the values given by the original authors. It thus appears that the variation from reaction to reaction, or energy to energy; shown in the figure more likely comes from systematic effects, rather than from a true variation of the emission region. As additional high statistics results become available, it will be of interest to analyze all experiments using the same method in order to search for true variations.

§4. Meson Resonance Production

This subject is closely related to that of clusters; indeed some of the clustering effects discussed previously must come from resonance production. There has been a controversy, however, as to whether resonances are a dominant or negligible effect in the cluster analyses.

The average number of ρ^0's per produced charged pion pair is shown in Fig. 8, taken from a compilation by Kenney *et al.* (paper 500); they find that at high energy about 12% of the produced charged pions come from $\rho^0 \to \pi^+\pi^-$. It should be noted that the ρ^0 signal is difficult to estimate due to the large combinatorial background. One might expect similar contributions from $\rho^{\pm}$ and from ω decays; further, the decays of η, K*, N*, and so on, will also contribute and thus the fraction of charged pions coming from resonant production and decay is probably 3 to 6 times larger than the 12% from ρ^0's alone. In fact, Dao *et al.* (paper 495) estimate that resonances can account for 80% of all charged pions in their pp data at 300 GeV/c. This can be compared with a recent estimate[9] that (10 to 30)% of the pions produced in 16-GeV/c π^+p interactions are "direct" and do not come from resonance decay.

At Fermilab-SPS energies only a small percentage of the ρ^0's come from diffraction dissociation (this process is only 10 or 20% of the total cross section and the multiplicity is low). Thus, the various estimates of 50 to 80% of the charged pions coming from resonance production must still be approximately valid for the high multiplicity events used to study clustering in the central region. This means that a majority of the so-called clusters are in fact old fashioned resonances, in which case "clusters" may not be the most appropriate language.

A compilation of the energy dependence for inclusive ρ^0, K*, and K_s production is shown in Fig. 9 (Kichimi *et al.*, paper 545); the figure shows that the inclusive production of ρ^0, K_s^0, and K_{890}^{*+} all scale together with energy, in approximately the ratio 1/0.6/0.3. The K^{*-} rises somewhat faster at lower energy and eventually becomes equal to K^{*+} above $\sim$50 GeV. These authors find that approximately two thirds of the K_s already come from K_{890}^* and K_{1420}^*, similar to the $\pi^{\pm}$ case where a large fraction also appears to come resonant production and decay.

Analyses of inclusive pion or kaon data is thus not at all straightforward. The contributions from resonance production and decay distort both the x distributions[9,10] and p_T

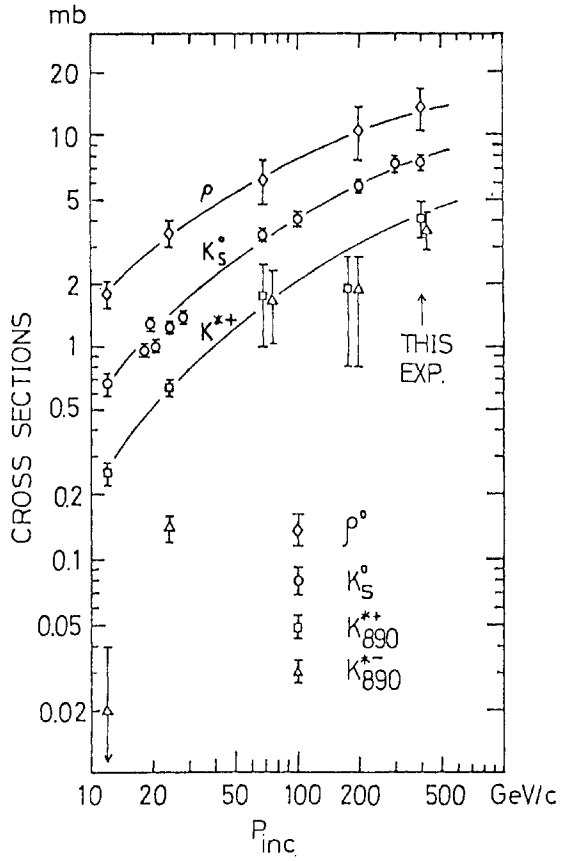

Fig. 9. Compilation of the inclusive cross sections for ρ^0, K_s and $K^{*\pm}(890)$ production in pp interactions (Kichimi *et al.* paper 545).

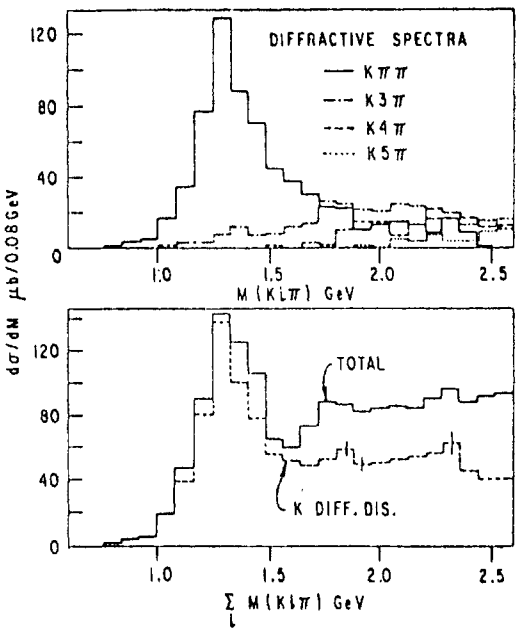

Fig. 10. The diffractive spectra for kaon diffractive dissociation: a) for different multiplicities; b) compared with the total apectrum (Morrison *et al.* paper 97).

distributions,[11] and can give misleading results if not taken into account in analyses such as triple Regge or parton fits. The x distortion caused by this effect depends on the process; one of the largest effects is that coming from ρ^0 decay contributing to $\pi^{\pm}\to\pi^{\mp}$.

We turn now briefly to the production of meson systems via diffractive dissociation. As is well known, this process gives a strong peak in the effective mass distribution near threshold. At larger masses the process becomes more difficult to identify, but Morrison *et al.* (paper 97) have developed a technique to identify the diffractive component using the energy dependence of the charge-exchange states to subtract off the non-diffractive part of the $\Delta Q=0$ states. Using this method they obtain a substantial diffractive component, even at the higher masses as shown in Fig. 10. For example, from their K^-p data at 10 and 16 GeV/c they find that at a K* mass of 2.5 GeV $\sim 1/2$ of the events come from diffractive dissociation. They obtain an integrated cross section $\sim 1.2\ \mu$b ($\sim 5\%$ of α_{tot}) each for diffractive K* and diffractive N* production.

§5. Triple Regge Phenomenology

Although several papers contributed to the Conference included triple Regge fits, I will have to limit myself to the recent experiment of Barnes *et al.* (paper 1065 and ref. 12) on π^0 and η production by 100-GeV/c $\pi^{\pm}$ beams. Not only do they have very high statistics, but they also have an interesting

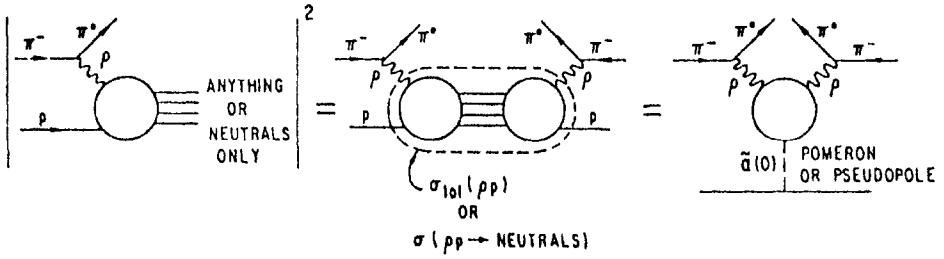

Fig. 11. Outline of triple Regge theory for $\pi^-p\to\pi^0X$ full inclusive and for neutrals only.

new twist to add to the game: using the same apparatus they did two experiments, first for the usual full-inclusive distribution and, secondly, for the zero-prong, neutrals-only final state. The theoretical models for these two cases are outlined in Fig. 11. For the full inclusive case one has the usual dominant term, Pomeron exchange at $t=0$ with $\tilde{\alpha}(0)=1$. For the neutral-only final state they introduce the concept of a pseudopole with trajectory at $t=0$ determined by the energy dependence of the zero-prong cross section (from which they estimate a value of $\tilde{\alpha}(0)=-0.08\pm0.2$). For each case they can then obtain the t depen-

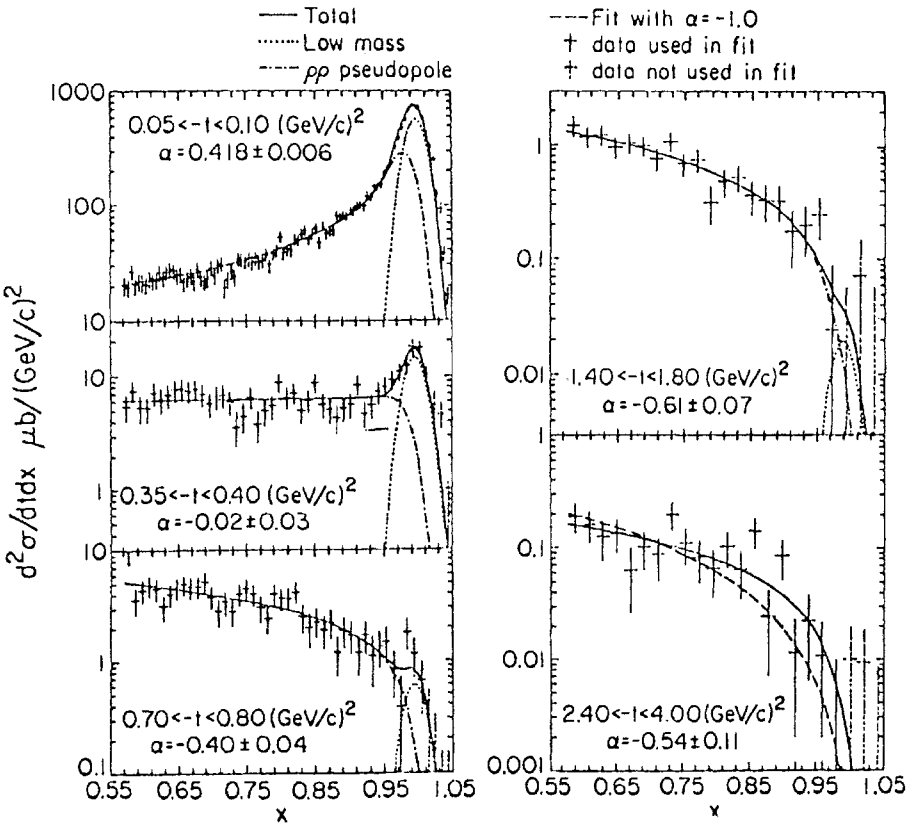

Fig. 12. The x dependence for $\pi^-p\to\pi^0$ plus neutrals only for different t bins, together with the triple Regge fits (ref. 12).

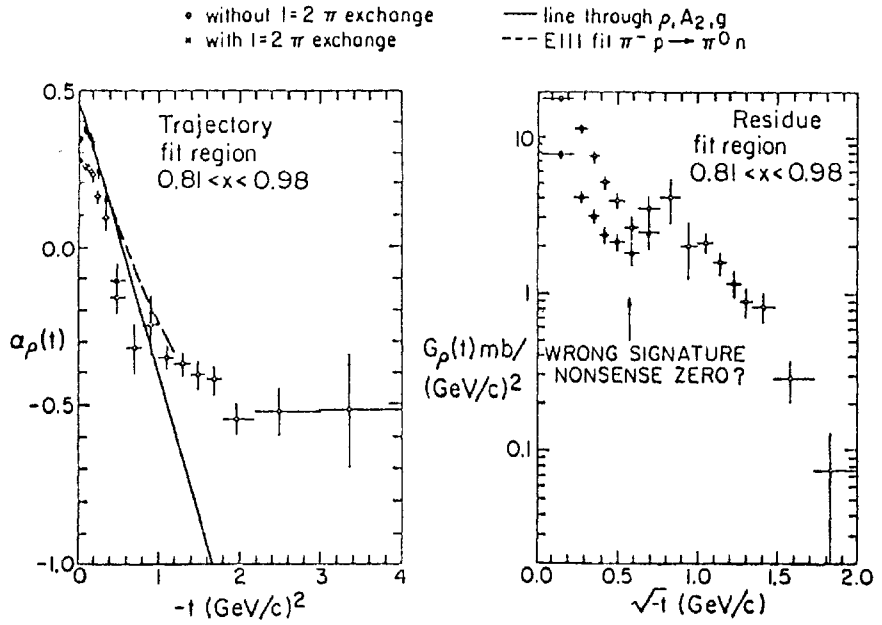

Fig. 13. The ρ trajectory and residue function found by fits to the full-inclusive π^0 data (Barnes *et al.* paper 1065), compared with the ρ trajectory from the exclusive data (ref. 13).

dence of the exchanged trajectory, $\rho(A_2)$ for $\pi^0(\eta)$ production, using the form

$$\frac{d^2\sigma}{dtdx}=f(t)\frac{(1-x)^{\tilde{\alpha}(0)-2\alpha\rho(t)}}{s^{1-\tilde{\alpha}(0)}}+\text{low-mass contribution from exclusive states} \tag{10}$$

A sample of the neutral-only inclusive data is shown in Fig. 12 together with the fit. Note that the shape of the spectrum does in fact change with t, as expected in the triple Regge model from the variation in $\alpha(t)$ with momentum transfer. The results for the π^0 full-inclusive case are shown in Fig. 13. The ρ trajectory is in qualitative agreement with that obtained[13] from the exclusive channel $\pi^-p\to\pi^0n$, while the ρ residue shows some structure in the neighborhood of $-t=0.5$ GeV^2, the exact nature of the structure depending somewhat on the details of the fit. Trajectories from the fits to the neutrals-only data are shown in Fig. 14.

The results of this work can be summarized as follows:

1. There is good qualitative agreement for the ρ^0 and A_2 trajectories obtained from the three final states:
   a) exclusive-neutron using energy dependence;
   b) full-inclusive using spectrum shape;
   c) neutrals-only using a different spectrum shape.
2. There are some systematic uncertainties from the value of $\tilde{\alpha}(0)$ used for the pseudopole and from the details of the fit (such as the x range used).
3. The trajectories appear to level off for momentum transfers >1.5 GeV^2 at $\alpha\sim -0.6$. This latter value can be compared with the constituent interchange model

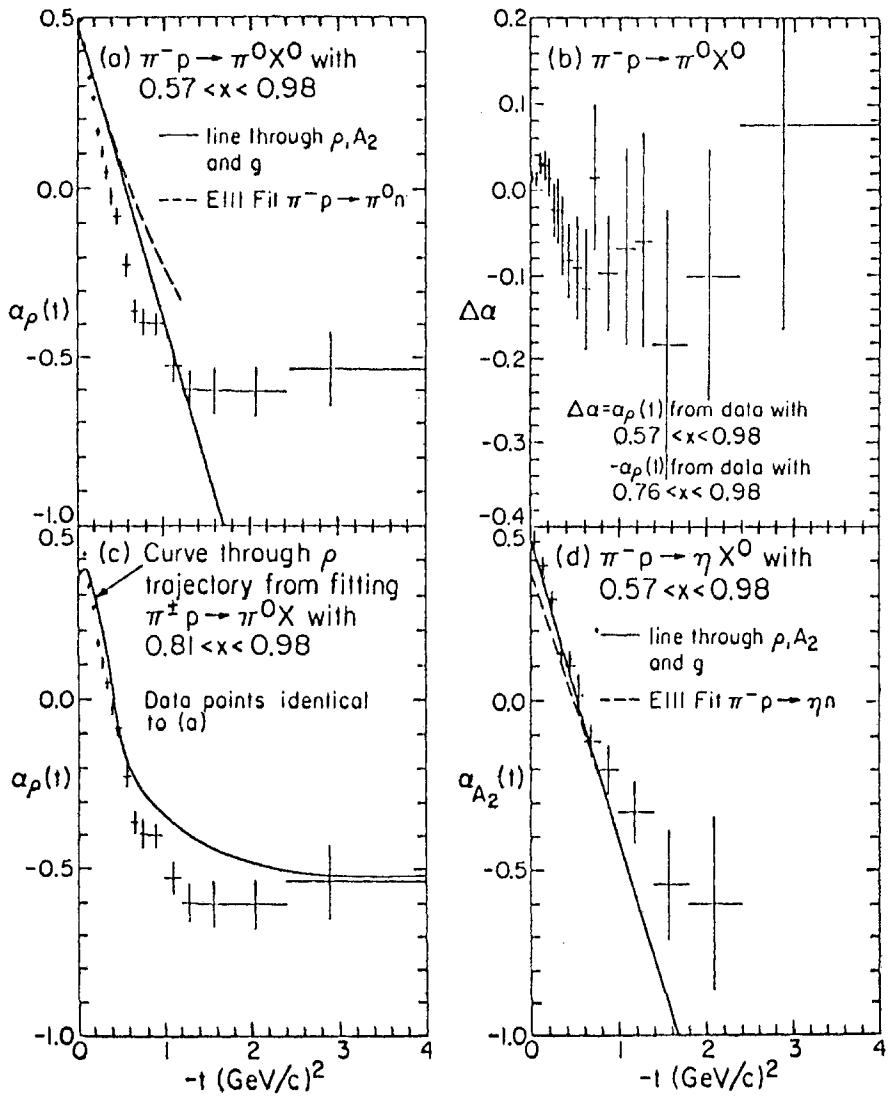

Fig. 14. The ρ and A_2 trajectories determined by fits to the neutrals-only data (ref. 13).

prediction of -1.

4. The ρ-exchange residues show structure (or a dip) near $-t=0.5\ \mathrm{GeV}^2$, whereas the A_2 residues are smooth in this region. The structre is presumably due to the wrong signature nonsense zero at $\alpha_\rho=0$.
5. From a detailed examination of their fits, the authors conclude that the simple Regge theory appears to work over a wider range of x for the neutrals-only final state as compared to the full-inclusive reactions. They suggest that this may be due to the weak coupling nature of the neutral final state and the corresponding pseudopole.

§6. Parton Ideas for Leading Particles

We turn now to a possible connection between low and high p_T phenomena. There has been a great deal of activity in this area during the last year or two, especially in explaining the momentum (or x) distribution of fast particles at low p_T with parton structure functions. The simple idea of fragmentation, sketched in Fig. 15a, does not work well; it gives too rapid a decrease in cross-section as x increases. The trouble is that momentum is lost at each of two stages: first, the single quark carries off only part of the initial pion momentum; and, secondly, it then fragments into the leading particle plus other particles which compete for momentum.

There are several ways to fix this; Andersson *et al.*[14] have suggested that the quark which interacts with the target is a wee quark with little momentum, leaving nearly the full energy for the fragmenting quark. Data presented to this Conference by the Fermilab Single Arm Spectrometer Group (Cutts *et al.*, paper 413), however, show that while this prediction gives approximately the correct shape for the x distribution, it generally does not have the correct normalization.

A more popular scheme is the recombination model sketched in Fig. 15b; this model assumes that the leading quark somehow dresses itself, or recombines, with a soft ($x_2\sim 0$) quark from the sea. This idea goes back several years[15] but received renewed interest from the observation of Ochs[16] that the ratio of π^+ to π^- inclusive production by protons follows very closely the ratio $u(x)/\mathrm{d}(x)$, where u and d are the quark structure functions found in deep inelastic lepton scattering. This idea has also been used successfully by Eisenberg *et al.* (paper 768) to fit the π^+/π^- ratio from similar reactions.

While Ochs neglected the momentum x_2 carried by the quark picked up from the sea, Das and Hwa[17] developed a model in which this x_2 distribution is folded in using a somewhat arbitrary recipe. This model has been used to estimate the sea-quark distributions

$$f_{\text{sea quarks}}\propto(1-x)^{n_q}. \tag{11}$$

Examples of such fits obtained by Duke and Taylor[18] are shown in Fig. 16. By fitting simultaneously to several particle ratios, they obtained both the shape and normalization of the sea-quark distributions. Similar fits have

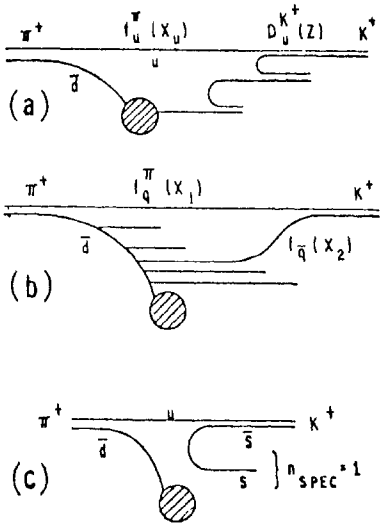

Fig. 15. Sketches of parton models used to describe low-p_T leading particles: a) fragmentation; b) recombination; c) spectator.

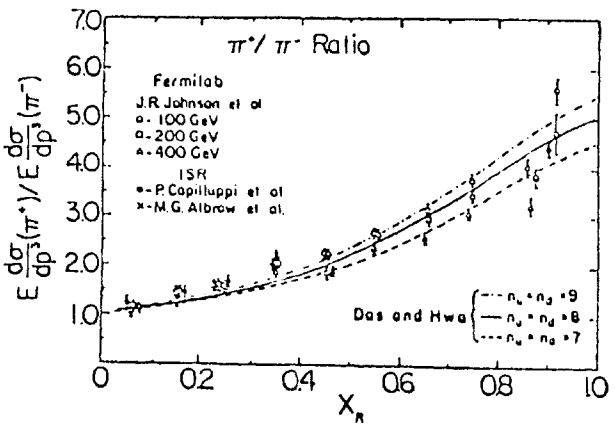

Fig. 16. Das–Hwa type fits to the $(p\to\pi^+)/(p\to\pi^-)$ ratio using several choices for the exponent in eq. 11 (ref. 18).

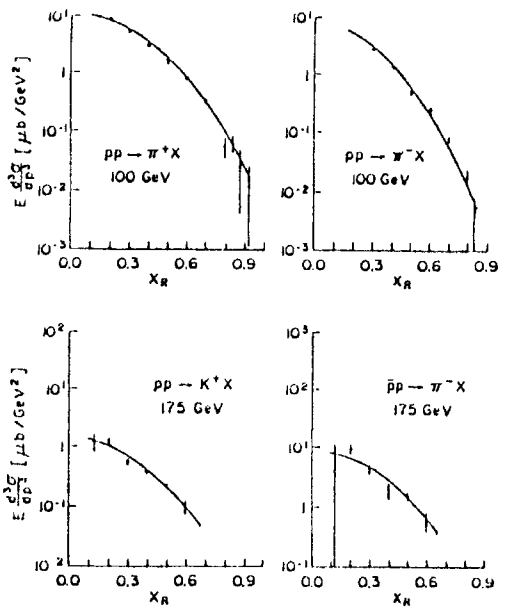

Fig. 17. Das-Hwa type fits to the invariant cross sections at $p_T=0.3$ GeV/c (D. Cutts *et al.*, paper 413).

also been obtained by the Fermilab Single Arm Spectrometer Group, Cutts *et al.* (paper 413), as shown in Fig. 17. Again, reasonable fits are obtained to the data by adjusting the parameters of the sea-quark distributions. The exponents in eq. 11 obtained for the sea-quark distributions from the two Fermilab experiments are as follows

	Cutts	Duke–Taylor
$\bar{u}$	7.5 ± 0.6	8 ± 1
$\bar{d}$	12.8 ± 2.3	
$\bar{s}$	6.5 ± 0.2	6 ± 2

There is good agreement between the two analyses, and the results are also in qualitative agreement with those obtained from dilepton production.[19]

Such fits have also been made[20] to the ISR data of the CHLM collaboration,[21] as shown

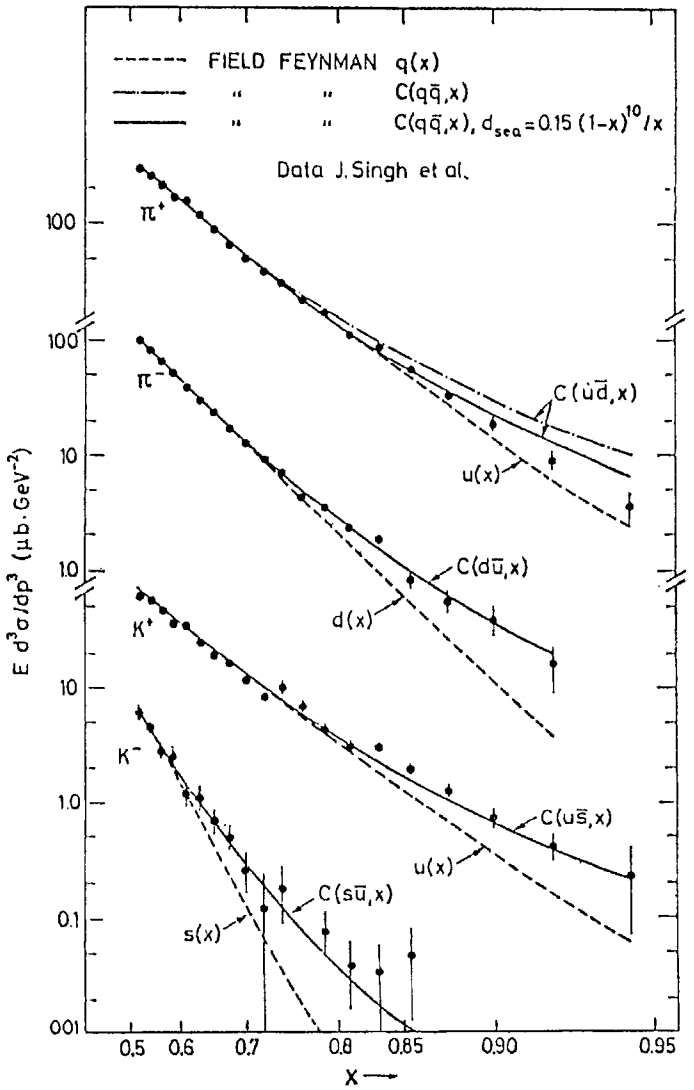

Fig. 18. Invariant cross sections for the production of particles in pp reactions at $\sqrt{s}=45$ GeV and $p_T=0.75$ GeV, compared with the appropriate quark distributions (dashed lines) and with the convoluted distributions (Das-Hwa); from ref. 20. Data from ref. 21.

in Fig. 18 for $p_T=0.75$ GeV/c. The dashed curves show the appropriate valence-quark distributions, and are the results one would obtain by neglecting the momentum contribution from the sea-quark. Better agreement with the data is obtained after convolution with the sea-quark distributions *à la* Das and Hwa.

In two papers presented to this Conference these ideas have been applied to data from incident pions and used to calculate the quark distributions within the pion:

Cutts *et al.* (paper 413)	Kenney *et al.* (paper 498)
valence$\propto(1-x)^{1.5\pm0.6}$	fix valence distribution to
nonstrange sea$\propto(1-x)^{3.0\pm0.3}$	various models, *e.g.*,
strange sea $\propto(1-x)^{0.9\pm0.3}$	Field–Feynman, then
	get sea $-(1-x)^{-4}$

The valence quark exponent of 1.5 ± 0.6 is in qualitative agreement with that obtained from the lepton pair experiments.[19]

These results should be taken with a degree of skepticism, however; it's amazing that the analysis works so well considering that:

1. The model is not well-founded on basic theoretical principles and is somewhat arbitrary (for example, the choice of the recombination probability to be x_1x_2/x^2).
2. The fits end up with so much momentum in the sea that there is none left over for gluons (compared with lepton scattering, hadron interactions take place over a relatively long time scale, and it is suggested in ref. 18 that the gluons convert their momentum into quark pairs during the interaction).
3. For some of these reactions there are substantial contributions from resonance production and decay which is usually not taken into account.
4. For some reactions triple Regge contributions are important.
5. Scaling violations and other gluonic effects inherent in the parton-quark model may mask the true quark distributions.

The problem of resonant production and decay has been particularly stressed by Pokorski and Van Hove.[15] The effect of ρ contributions to the $p\to\pi^{\pm}$ inclusive spectra has been examined by Erne and Sens;[20] they find that while the effect is not dominant, it could well affect detailed quantitative fits such as those done to obtain the sea quark distributions.

The same data have been fit[21] for $x>0.7$ to the triple Regge model; the resulting Regge trajectories are shown in Fig. 19. The reactions $p\to\pi^+$, π^-, K^+ all give similar values for $\alpha(t)$, even though somewhat different values were expected for the different reactions. Perhaps one should simply be pleasantly surprised that the fits gave answers this close, since the inclusive production is a sum of not only triple Regge type terms, but also parton type processes, as well as resonance production and decay.

In spite of the complexity of low p_T physics the parton concepts do appear to be useful for an intuitive grasp of the data. For example, we can ask what happens to the π^+/π^- ratio, so beautifully explained by Ochs,[16] if we now require also an additional fast π^-. Naively, one might have thought the ratio would remain invariant under the requirement of the extra π^-; however, the first π^- uses up the only d valence quark in the proton and for the second π^- both the quark and anti-quark must come from the sea. This requirement is similar to that for K^- production, and as shown[22] by Fig. 20 the $\pi^+\pi^-/\pi^-\pi^-$ ratio is

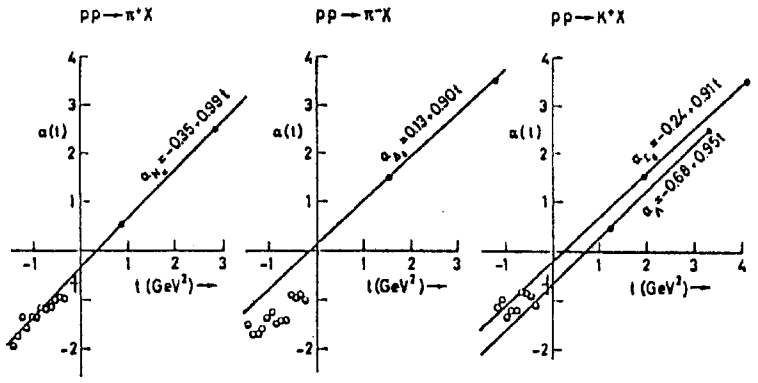

Fig. 19. Effective trajectories from one-term triple-Regge fits to the region $x>0.7$ (ref. 21).

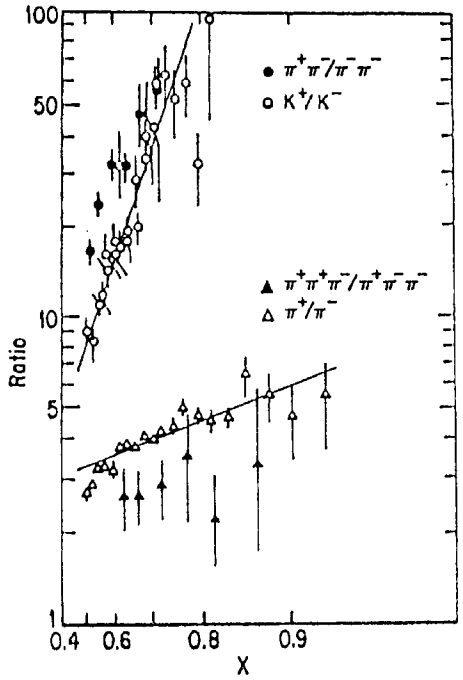

Fig. 20. Cross section ratios from pp interactions at $\sqrt{s}=53$ GeV (ref. 22).

indeed in qualitative agreement with the K^+/K^- ratio. Other situations of this sort can also be studied; for example, the π^+/π^- ratio has been predicted[23] to change dramatically for events which contain lepton pairs of high effective mass. In the Drell–Yan model such pairs will be made preferentially by $u\bar{u}$ annihilations which would then leave behind a different distribution of quarks available for hadron production.

An alternative, more superficial method for estimating the leading particle momentum distributions is given by the spectator counting rules of Brodsky and Gunion.[24] The best results are obtained if one assumes that one of the beam quarks is absorbed on the target, and the produced particle is accompanied by the minimum number of spectator quarks, as shown, for example, in Fig. 15c. Since the momentum must be shared with these spectators, one expects for the fast particles

$$x(\mathrm{d}\sigma/\mathrm{d}x)\propto(1-x)^{2n_{\mathrm{spec}}-1}. \qquad (12)$$

This is obviously a cruder model then those discussed previously. For example, both π^+ and π^- produced from incident protons would then be expected to go as $(1-x)^3$, whereas it was the ratio of these two reactions which was fit so well by Ochs using the difference between the u and d quark valence distributions.

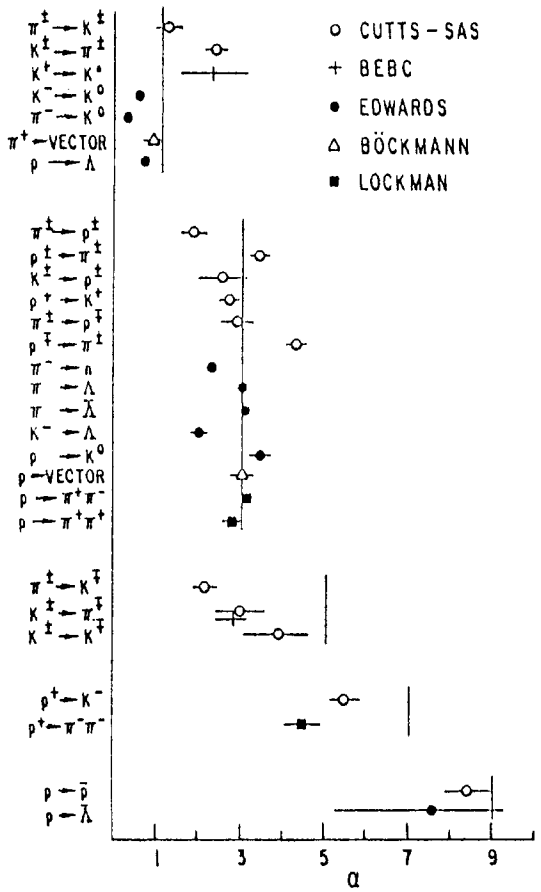

Fig. 21. Compilation of the exponent α used to characterize the dependence of inclusive processes at large x; $x\mathrm{d}\sigma/\mathrm{d}x=(1-x)^{\alpha}$. The data come from the sources listed in ref. 25 and are compared to that expected by spectator counting in the quark exchange model (ref. 24).

In Fig. 21 I have compiled some of the recent experimental results[25] and compared them with the predictions of the spectator counting model. At best, the model gives a rough measure of the difficulty in creating a fast particle of a given type. While some reactions are described well, others miss by one or sometimes two units in the exponent. Since the data are typically being fit over a range in $1-x$ of a factor of five, this means that the model often gives a fall off which disagrees with the data by a factor of 5 to 25. The model is particularly unreliable for those processes with three or four spectator quarks. In some cases one can make excuses based on resonant contributions, triple Regge effects, helicity flip dominance, etc., but this means that the predictive power of the modelis limited.

Some of the worst disagreements with the spectator quark counting rules are shown by the recent SPS hyperon beam results (Bourquin

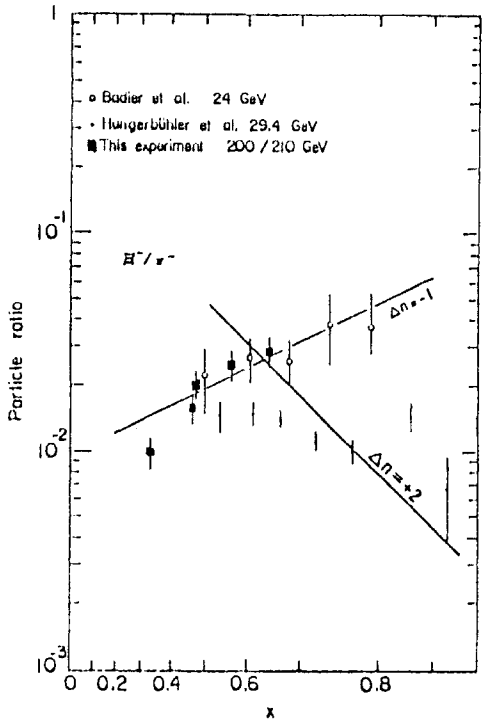

Fig. 22. Ratio for Ξ^-/π^- produced in the forward direction by protons (M. Bourquin *et al.*, paper 777).

et al., paper 777) such as the Ξ^-/π^- ratio shown in Fig. 22. While the previous low-energy experiments disagree with one another, it is clear that this ratio is far from compatible with the prediction of the spectator model.

§7. Heavy Stable Particle Surveys

Here we will discuss the production of particles with lifetime sufficiently long to be observed in a secondary beam. We begin with three experiments which looked in vain for particles with mass in the region of 5 GeV. While it is always good to look for new effects on general principles, these experiments are of particular interest in view of the speculation by Cahn[26] that the new quark in the Υ might form stable or highly metastable compounds with the lightest of the old quarks, yielding a relatively stable meson with mass in the region 5 GeV. Two Fermilab experiments were performed recently with the parameters and results outlined in Table I. The Single Arm Spectrometer results of Cutts *et al.* are somewhat more sensitive, setting a 90% confidence upper limit roughly 20 times smaller than that for Υ production. The results of Bourquin *et al.* (paper 777) using the SPS charged hyperon beam are also shown in Table I. While their cross section limit is several orders of magnitude less stringent than those of the Fermilab experiments, they are able to see down to lifetimes of order 10^{-9} seconds; again, no significant signal was observed.

The beam survey experiment of Bozzoli *et al.* (paper 915 and reported by Giacomelli in section A3) also searched for particles with lifetimes $>10^{-8}$ seconds. They were able to set upper limits on the flux of such particles, $<10^{-7}$ that of pions for new particles with $M<1$ GeV; at higher masses, 3–10 GeV, the limit is of order 10^{-10} of pion flux. This group also measured the flux of light nucleons and anti-nucleons. As one tries to make more and more nucleons (or antinucleons) stick together the cross section falls rapidly, the price being a factor of 2,000 per nucleon and 6,000 per anti-nucleon. These results can be compared with the sticking model which predicts

$$\sigma_{\bar{d}}/\sigma_d \approx (\sigma_{\bar{p}}/\sigma_p)^2. \tag{13}$$

The observed $d/\bar{d}$ ratio is actually found to be three times this prediction.

The last experiment of this type which I

Table I. Searches for quasi-stable particles of $M \approx 5$ GeV; upper limits are 90% confidence level.

	Cutts *et al.*, RPL 41, 363 (1978)	Vidal *et al.*, Fermilab-Pub 78–48	Bourquin *et al.*, Paper 777
Primary beam-target	pBe	p(BeO)	p(BeO)
Primary, secondary mom. (GeV/c)	400→−70	400→−70	200→±95
Beam line	M6+SAS	N1	SPS Chgd. Hyp.
Length (m)	500	920	10–30
τ for $e^{-2.3}=1/10$ (sec) at $M=5$ GeV	0.6×10^{-7}	1×10^{-7}	$\sim0.7\times10^{-9}$
No. of Cerenkov counters	8	2	3
Mass range searched (GeV)	4 to 10	4.5 to 6	2 to 10
Number of light particles	10^{11}	0.5×10^{11}	$X^{\pm}/\pi^{\pm}\leq10^{-7}$
$E(d^3\sigma/dp^3)(\text{cm}^2/\text{GeV}^2)$	$<1.1\times10^{-37}$	$<3\times10^{-37}$	

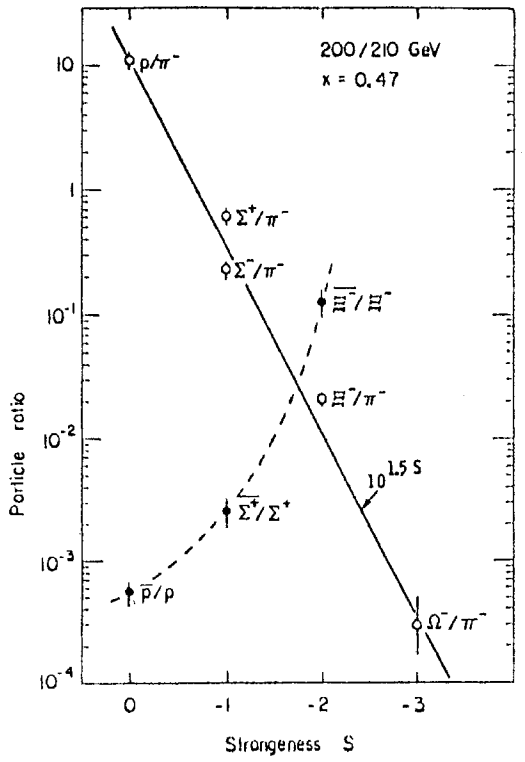

Fig. 23. Particle producton by protons as a function of S (M. Bourquin *et al.*, paper 777).

shall discuss is the survey of charged hyperons from 200 GeV interactions shown in Fig. 23. Here one pays a price of a factor of 30 in rate for each unit of strangeness. Note the rapid increase in the anti-baryon to baryon ratio as the strangeness increases; for $S=2$ the ratio is already $<10\%$, leading one to speculate that the ratio of anti Ω^-/Ω^- may be close to unity.

§8. Non-Emulsion Searches for Charm

In a previous section we considered inclusive production of some of the old meson resonances; in a similar vein this section considers the inclusive production of charm resonances by hadron beams. This subject is obviously important since inclusive charm production gives another dimension to the study of dynamics, namely, the production of massive quarks or particles which can be compared with that of the lighter particles.

A list of some of the non-emulsion charm searches[27] is given in Table II; in general, I have limited myself to experiments well above threshold, $\sqrt{s}>10$ GeV. One must treat the cross sections listed in the table with caution. In general, the experiments are sensitive to only a small fraction of the 4π solid angle, and a large extrapolation must be made using some theoretical model; different models have been used by the different groups. Further, the A dependence assumed for production off nuclei is often not mentioned and this can lead to an uncertainty of a factor of three in the cross section extrapolated to hydrogen. Also, it is sometimes not clear whether the cross section limit being quoted is for all D's, or only for a particular charge state, or whether the cross section is

Table II. Non-emulsion searches for inclusive charm production; limits are generally 95% confidence level on statistics, but do not include the systematic uncertainties of typically a factor of three.

First author	Decay modes	Reaction	$\sqrt{s}$ GeV	$\sigma(pp\to DDX)$ μb/nucleon
Antipov	$K\pi$; $K\pi$	π^-Be	10	<(2–9)
	$K\pi$; μ			<(10–20) (A^1)
Albrecht	$K^0\pi^\pm$ (or $K\pi\pi$)	nC	10	$<\sim 25$
Jonckheere	μ; μV^0	π^-C	20	<22 (A^1)
Abolins	$K\pi$	nBe	22	<15
Spelbring	$K\pi$; μ	nBe	24	<100 ($A_{\rm eff}=6.4$)
Lipton	$e^\pm$; $\mu^\mp$	nBe	24	<30 ($A_{\rm eff}=6.4$)
Lauterbach	μ	pCu	27	$<\sim 1$ (using longit. pol.)
				$<\sim 10$ (without pol.)
Ditzler	$K\pi$	pBe	27	<30
Baum	$e^\pm$; $\mu^\mp$	pp	55	<76
Clark	$e^\pm$; $\mu^\mp$	pp	55	76 ± 36
				25 ± 10
Brown	single μ	pFe	27	30–80 (A^1)
Soukas	beam dump→ν	pCu	7	1
Asratyan	beam dump→ν	pFe	12	19 ± 15
Hansl	beam dump→ν	pCu	27	40
Alibran	beam dump→ν	pCu	27	100–200 ($A^{0.7}$)
Bosetti	beam dump→ν	pCu	27	100–200 ($A^{0.7}$)

per D meson or per pair of D mesons. Thus the upper limits quoted generally have systematic uncertainties of a factor of three or more. In making the table, I have normalized the results to a set of standard branching ratios.[28]

The experiments range from those with a good direct signature, such as searches for bumps in the mass spectrum of $K^+\pi^-$, to those where the signature is rather indirect. Unfortunately, those experiments with potentially good signatures observe no conclusive evidence for charm production by hadron beams; in general, the upper limits are in the neighborhood of 10 to 20 μb. The upper limit of Lauterbach is only 1 μb, but this result is model dependent since it assumes that the muons from semi-leptonic D decay have a high longitudinal polarization; if this polarization information is ignored, the upper limit is of order <10 μb. Another of the more indirect experiments (Clark *et al.*, paper 115) looks at eμ pairs at the ISR, and claims to see a two standard deviation effect after a large background has been subtracted.

Recently, two types of experiments have observed significant signals. Brown *et al.* (paper 1011) run a proton beam into a large hadron calorimeter and observe events with *single* muon production. After correcting for the decays in flight of pions and kaons they conclude that they are observing a cross-section in the region 30–80 μb (under the assumption of an A^1 dependence). At the present time the most straightforward explanation of the single muon events would be the production and semileptonic decay of charmed particles. However, the cross-section quoted is larger than the upper limits set by many of the previous experiments.

The SPS neutrino beam dump experiments observed signals consistent with the production and fast decay of charmed particles in the beam dump, although the three experiments disagreed on the size of the effect, with cross sections for charm production now quoted from 40 to 200 μb (under the assumption of an $A^{0.7}$ dependence). Again, these cross sections seem high when compared with the upper limits obtained by the other experiments listed in Table II; the disagreement can be reduced if an A^1 dependence is assumed, in which case the cross sections would fall in the range 10 to 50 μb. For comparison, the 28-GeV/c beam dump experiment at Brookhaven of Soukas *et al.* (paper 1156) set an upper limit of ~ 1 μb.

A search for charm was carried out in BEBC by looking for prompt single electron (or positron) production by 22-GeV/c π^- in hydrogen (Calligarich *et al.*, paper 1150). Out of 25896 interactions they found one unambiguous event of this type:

$$\pi^- p \to e^- K_s^0 \pi^- \pi^+ (K^+) \gamma p X^0$$

where X^0 is the unobserved system of neutral particles (missing mass ~ 1.4 GeV). The presence of the K_s^0 suggests that this could well be charm production. The one event corresponds to $\sigma \times BR \approx 1$ μb (10 μb for a 10% semileptonic branching ratio).

Albrecht *et al.* (paper 149) used a Serpukhov wire spark chamber spectrometer to look at 45 GeV nC interactions and have found the

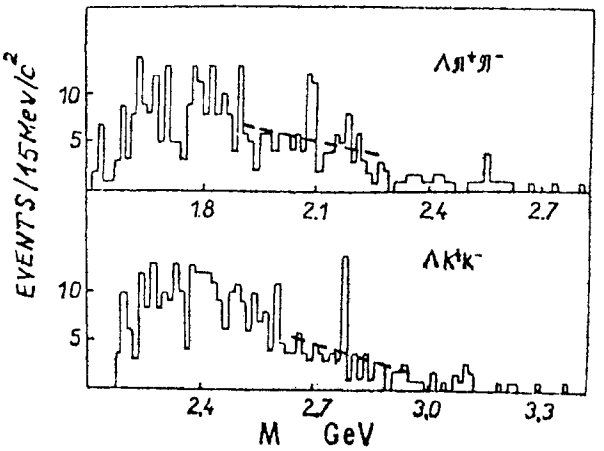

Fig. 24. Invariant mass distributions from 45-GeV nC interactions (Albrecht *et al.*, paper 149)

two narrow bumps in Fig. 24. The first bump is seen in the $\Lambda\pi^+\pi^-$ system at a mass of 2085 MeV, 23 events compared with ~ 10 expected. The second bump is in the ΛK^+K^- mass spectrum at 2790 MeV; 13 events compared to ~ 4 expected. These bumps could be interpreted as decays of charmed baryons, but with ~ 4 standard deviations per bump they clearly need confirmation; the authors quote a $\sigma \times BR \sim 1$ μb/nucleon each.

While bare charm is indeed proving difficult to observe in a reliable manner with hadron beams, hidden charm in the form of ψ and ψ' has been observed over the years and I have nothing qualitatively new to report here.

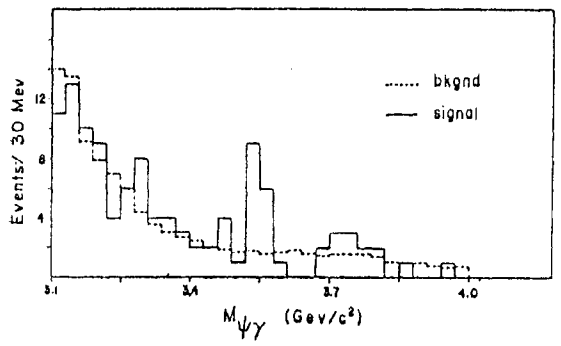

Fig. 25. The $\psi\gamma$ mass spectrum produced by a beam of 215 GeV/c π^-; the background distribution was generated by taking uncorrelated ψ's and γ's (Holloway *et al.*, paper 440).

Since the Υ is discussed in the talk of Lederman, I will not discuss it either. The one piece of hidden-charm physics that I do want to discuss is shown in Fig. 25. The Fermilab Chicago-Cyclotron-Magnet Spectrometer was used by Holloway *et al.* (paper 440) to observe the production of χ states by a 215-GeV/c π^- beam. They find events with $\psi\to\mu^+\mu^-$ and then look for an additional γ ray; the $\psi\gamma$ mass distribution shows a bump of 11 ± 4 events at 3550 MeV. This is just the mass of one of the χ states and after correcting for their γ-ray acceptance they find that $(38\pm 13)\%$ of the ψ's are produced *via* $\chi(3555)$ production and decay. This number compares well with the value $(43\pm21)\%$ observed previously at the CERN ISR by Cobb *et al.*[29]

§9. Short Lived Particles in Emulsions

The observation of production and decay of charm particles in emulsion should have the advantage of a clean signature and of relative independence of decay modes. Such experiments do depend, however, on possible biases and the lifetime; indeed, measurements of the lifetimes of charmed particles are also of great interest. In a simple, bare emulsion experiment one would actually observe the superposition of several different lifetimes from the different charm particles. In principle, this problem is avoided by some of the newer experiments which back up the emulsion stack with a large spectrometer or bubble chamber, both to locate interesting events in the emulsion and to separate the different charm particles through their decay products. Other uncertainties in the lifetime measurements come from possible scanning biases, both at very short and very long distances, as well as from the estimate of the Lorentz factor $\gamma=E/M$.

A list of emulsion experiments is shown in Table III. Several of these experiments have been presented to this Conference and claim

Table III. Some emulsion experiments on short-lived particles.

Paper	Beam	Comments	Events/Interaction	σ (μb/nucleon)	τ (10^{-13} sec)
Bannik *et al.* (paper 154)	70 GeV p 60 GeV π^-	only search $l\leq100$ μ	4 events/$\sim$20000 ints. (each with an electron)	5 ± 3	~0.6
Coremans-Bertrand *et al.* PL **65B**, 480 (1976)	300 GeV p	first decay <150 μ, second <2 mm	no pairs/60000	<1 1/2 90% conf. ($A^{2/3}$)	—
Bozzoli *et al.* L. N. Cim. **19**, 32 (1977)	300, 400 GeV p	first decay 10 to 600 μ second <2 mm	no pairs/16000	<7	—
Ushida *et al.* (paper 492)	400 GeV p	first decay at 320 μ, second at 2930 μ	one pair/312	~30	~1
Chernyavsky *et al.* (paper 308)	400 GeV p	search ≤1 mm	9 singles/1120	~120 (A^1)	~0.2
Fuchi *et al.* (paper 491)	10–20 TeV	cosmic ray compilation of assoc. prod.	1 pair or cascade per 20–40 ints. (20 decays observed)	~500	$X^0\sim4$ $X^\pm\sim12$
Diambrini-Palazzi	20–80 GeV γ	<3 mm (along relativistic tracks)	2 possible singles (16, 30 μ)per 482 ints.	$\sim1/2$	0.02–0.05
Burhop *et al.* PL **65 B**, 299 (1976)	ν	broad-band beam from 400-GeV p	1 single/16 ints.		~6
European ν Collab. (paper 798)	ν	broad-band beam from 350-GeV p	0/31 charged current ints.		—

to have positive results. In general, these positive results are in contradiction to the upper limit $\sim 1\ \mu$b set by the two earlier experiments listed in the table, which were unable to find associated pairs in a search of the region down-stream of 76,000 primary interactions.

Two new experiments claim to have seen short-lived decays, based on the observation of single decays. In an experiment performed at Serpukhov Bannik *et al.* (paper 154) have observed four events having an electron associated with the secondary vertex. While Gaisser and Halzen[30] have estimated that backgrounds in single-decay samples (from interactions and decays of non-charm particles) are expected at the few to 50% level, Bannik *et al.* claim that the requirement of an electron should result in a very small background.

Chernyavsky *et al.* (paper 308) have found nine charm candidates out of 1120 primary stars produced by 400-GeV/c protons. Although they scan out to 1000 μ these events show flight paths of only 12–90 μ. With such short flight paths there should be little probability of background from interactions. Their integral distribution of lifetimes is shown in Fig. 26. As indicated by the straight line, a lifetime in the neighborhood of 2×10^{-14} represents the data well; the systematics on such a lifetime may be large, however, due to possible scanning biases. These authors suggest a reason for the nonobservation of associated events: perhaps charm production proceeds mainly through associated production of a charmed meson together with a charmed baryon, the meson having a lifetime too short to be observed reliably in the emulsion. Indeed, for most of these nine events one must assume that the observed decays are of baryons, rather than mesons, if the mass is to be in the neighborhood of 2 GeV.

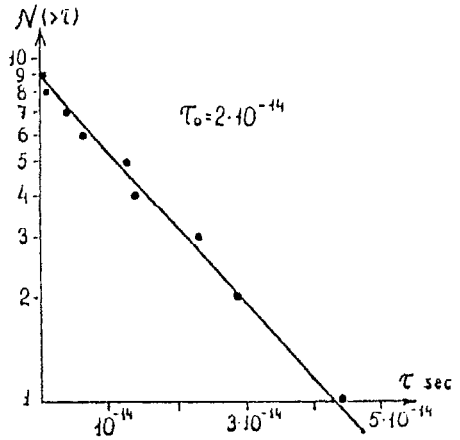

Fig. 26. Integral distribution of the lifetimes of the nine short-lived particles observed by Chernyavsky *et al.* (paper 308). The lifetime value shown should be considered preliminary due to possible scan biases.

Still, this does not explain why the two earlier experiments with much higher statistics did not observe such events. Although these earlier groups emphasized their nonobservation of associated pairs, in fact they also looked at single production and found only a few events, consistent with the flat lifetime distribution expected from interactions or hyperon decays. For example, Bozzoli *et al.* only observed 8 events with decay paths <100 μ's even though they looked at 15 times as many interactions as Chernyavsky *et al.*

Fuchi *et al.* (paper 491) have made a compilation of short-lived particles produced by cosmic rays in the energy region 10–20 TeV. To reduce backgrounds they accept only events having two or more short-lived particles. Out of six intereactions, some of them from exposures 20 or 30 years ago, they find 20 candidates. The integral lifetime spectra for both charged and neutral candidates are shown in Fig. 27. The six neutral short-lived particles suggest a lifetime in the neighborhood of 0.4×10^{-12} seconds, while the 14 charged particles give a lifetime of roughly 3

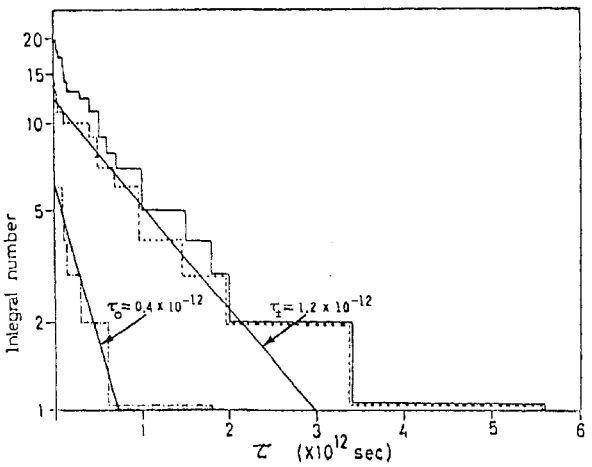

Fig. 27. Integral lifetime distributions for short-lived particles from associated production by cosmic rays of 10–20 TeV; solid line shows charged plus neutral particles, dashed line for charged, dash-dot for neutrals. No correction has been made for scan biases. Compilation by Fuchi *et al.* (paper 491).

times as long. It is interesting to note that Fig. 27 is consistent with the theoretical suggestion[31] that the lifetime of the charged D meson is longer than that of the neutral. The authors estimate that short-lived particles are produced every 20–40 events at these energies, *i.e.*, a cross section of ~ 500 μb/nucleon.

For completeness, Table III also shows results obtained from γ-ray and neutrino interactions in emulsions. The results of the Omega Photon Emulsion Collaboration were presented in session B4 by Diambrini-Palazzi. So far, they have found two possible candidates, both with rather short flight paths, suggesting a lifetime of $<10^{-14}$ seconds. While one event was found in a previous neutrino emulsion experiment, the most recent experiment (paper 798) has thus far been unable to find any candidates in a search of 31 charged-current interactions. As with the γ-ray experiment, this latter neutrino experiment has really only begun the long and tedious task of scanning, so additional results can be anticipated within the next year or two; other emulsion experiments are being set up at Fermilab as well.

I would now like to summarize the present inclusive charm situation. Can all of these experiments be consistent with one another? With enough *ad hoc* assumptions one could probably get consistency between the majority of the experiments; however, my guess is that at least some of them are wrong or have been given a wrong interpretation. One of the worst discrepancies is between the old high-statistics emulsion experiments and the more recent beam dump experiments. This has been investigated in some detail by Crennell *et al.*[32] who combine the $D\bar{D}$ production model of Halzen and Matsuda[33] with the scan criteria of the Coremans–Bertrand experiment. They conclude that the experiments could be consistent if the average lifetime of the charmed particles were either $<0.5\times10^{-31}$ or $<10^{-12}$ seconds. This can be compared with the theoretical expectations[31] of 0.5×10^{-12} seconds; the theorists claim they would be surprised if the lifetime lay outside the range 10^{-14} to 10^{-11} seconds and this would prejudice one against the very fast lifetime possibility. The lifetime cannot be much more then 10^{-12} seconds, however, or various bubble chamber experiments would have been able to detect the finite decay length. Since both the emulsion experiments and beam dump experiments assume the same A dependence, this possible systematic error cannot explain the discrepancy between the two experiments. If the charm particles were produced more diffractively, a smaller cross section could produce the observed number of neutrino interactions from the beam dump experiments. Much more than a factor of 2 or 3 is improbably, however, because the neutrino spectrum would then disagree with that observed.[34] Systematic errors of a more experimental nature are also possible, of course, and are even strongly suggested by the fact that neither the emulsion experiments nor the beam dump experiments agree well amongst themselves.

More exotic explanations are also possible, although these are perhaps premature. One possibility would be that the neutrinos in the beam dump experiments originate primarily from the decay of some other type of particle, such as mesons with one of the new Υ quarks. Another possibility suggested to this Conference (Banerjee and Subramanian, paper 437) involves new, relatively-light neutral bosons produced in pairs with a small cross section and long lifetime.

My own guess is that the charm cross section at Fermilab–SPS energies is of order 10 μb/nucleon with lifetimes hiding in the shadows near 10^{-12} seconds. With all of the present experimental effort being brought to bear on this problem, it should be well understood by the time of the next Conference.

§10. Centauro Events

The only way to study interactions above $\sqrt{s}=60$ GeV at present is to use cosmic rays. Although these experiments are very difficult, they have over the years indicated the trends to be expected at higher energies. Rising total cross sections, the increase in transverse momentum, and a rapid increase in average multiplicity have all been shown by these experiments. Rather than trying to cover all of the results from the cosmic ray experiments, I will concentrate instead on one topic, the so-called Centauro events.

While such events are not observed at present day accelerator energies they are

apparently produced relatively frequently, at least a few per cent of the total cross section, at lab energies of 1,000 TeV. They are characterized by a high multiplicity of strongly interacting particles, roughly 80, but are consistent with having no γ rays, and thus no π^0's, coming from the primary interaction. Five such events have been observed by a Brasil–Japan collaboration (paper 434) using emulsion chambers on Mount Chacaltaya in Bolivia, 5200 m above sea level.

These interactions take place in the atmosphere, typically a few hundred meters above the apparatus. Only the height of the first event could be measured directly; it was found to be 50 m above the apparatus and gave an average p_T of 1.7 ± 0.7 GeV/c. The heights of the other events have been calculated assuming the same average transvrse momentum. The characteristics of these events are outlined in Table IV.

Table IV. Characteristics of the Centauro and Mini-Centaruo events (Brasil-Japan Collaboration, paper 434).

	Centauros	Mini-Centauros
No. events	4+1	13
Interaction height (m)	50, 80, 230, 500	300–1900
Hadronic mult.	70–90	~15
Fireball mass (GeV)	~200	~30
Total energy (TeV)	1000–1400	250–2500

It was found that the energy and transverse momentum of the secondary particles are exponential and that the angular distributions are consistent with isotropy, making it natural to speak of the production of a fireball. They have calculated the mass of the fireball using two methods, each giving $M\approx200$ GeV. The first method uses the average transverse momentum to deduce the average energy in the center of mass to be 2.3 GeV per particle; the mass of the fireball is then just calculated as the number of particles times this average energy. The second method assumes a forward-backward symmetry in the center of mass system; the median angle, θ_m, then corresponds to 90° in the center of mass and the mass can be simply calculated as

$$\tan\theta_m=\frac{p_T}{p_\parallel}=\frac{p_T^*}{\gamma\beta E^*}\approx\frac{1}{\gamma}=\frac{M}{E}$$

$$M\approx E\theta_m$$

where E is the total laboratory energy of the fireball. This energy is measured in the emulsion chambers by allowing the particles from the Centauro events to interact in the apparatus, converting about one-fifth of their energy to π^0's, the γ rays of which can be measured in the emulsion chambers. They then observe a sum of γ-ray energies, $E_{\rm obs}\approx$ 200 to 300 GeV, implying a total energy for these events in the neighborhood of 1,000 to 1,400 TeV, and this result gives a fireball mass quite consistent with that obtained by the average transverse momentum.

As shown in Table IV, these authors have now also observed 13 events which they call mini-Centauro. While these events only have ~15 strongly interacting particles, a somewhat low multiplicity, they share with the Centauro events the characteristic of having little or no γ rays from π^0's.

While the Centauro events need confirmation from other experimental groups, their presence could help to explain some of the other effects such as high multiplicity and large average transverse momentum seen by the various cosmic ray experiments. The colliding beam projects being planned for the next few years at CERN, Fermilab, and Brookhaven will probably have sufficient energy to observe this new type of interaction; for example, $\sqrt{s}=$ 800 GeV corresponds to a laboratory energy of 340 TeV. With their large cross section such events should be relatively easy to see, even at the low luminosities which may be present during the initial operation of these colliding beam systems. Whether or not the Centauro events are eventually confirmed, they do hold a lesson for us as we seek to expand our energy horizons with accelerators: we should not simply imagine that nature continues on in a unimaginative and dull lns fashion; she may in fact have some real surprises up her sleeve, in this case a totally new type of strong interaction setting in above some high-energy threshold. Judging from the high multiplicities observed in extensive air showers at even higher cosmic ray energies, more than one surprise may be waiting for us.

§11. Interactions Off Nuclei

There has been considerable work, both experimental and theoretical, in this field,

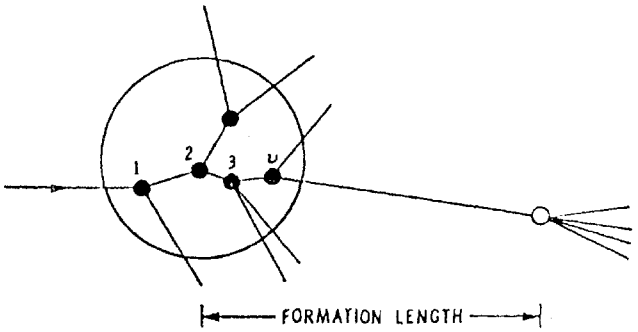

Fig. 28. Schematic view of interactions in nuclei.

particularly in the Soviet Union. Here I will mention just a few of the points to give a flavor of the physics and to remind those not working directly with nuclei of this very active sub-culture.

A simple, naive picture of an interaction in a nucleus is shown in Fig. 28. Experiment shows that the fast, high-energy stuff acts much like the incident beam particle while inside the nucleus. In particular, there is very little cascading of the sort observed in a hadron calorimeter, where the first interaction might produce 10 particles, each of which in turn interact to produce several more particles, and so on, leading to a rapid build up of the shower. This is not observed. If we define ν_p to be the number of interactions of an incident proton in the nucleus, then the average number can be expressed as

$$\bar{\nu}_p \approx A\sigma_{\text{inel}}(pp)/\sigma_{\text{inel}}(pA) \approx 0.7\,A^{0.3} \tag{14}$$

The number of fast charged secondaries coming from nuclear reactions normalized to those from hydrogen,

$$R_A = \langle n\rangle_A / \langle n\rangle_{\text{hydrogen}}, \tag{15}$$

is plotted in Fig. 29 (ref. 35) as a function of both $A^{1/3}$ (proportional to the nuclear radius) and the variable $\bar{\nu}$. As shown by the figure, the data lie on the straight line

$$R_A = 0.47 + 0.61\,\bar{\nu} \tag{16}$$

when plotted as a function of $\bar{\nu}$, but do not show a simple relationship when plotted as a function of the nuclear radius. This result shows a surprising simplicity of these high energy interactions: the high-energy stuff propagating through the nucleus acts much as the beam particle itself, even though ti becomes an exicted system which eventually decays out-

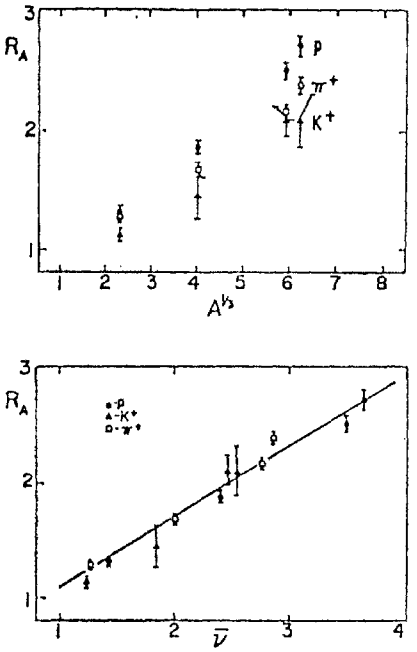

Fig. 29. Charged particle multiplicity ratio (eq. 15) at 100 GeV/c as a function of $A^{1/3}$ (proportional to the nuclear radius) and $\bar{\nu}$ (eq. 14); from ref. 35.

side the nucleus. Dimensional arguments give for this decay or formation length

$$l \sim p/(M^2 + P_T^2), \tag{17}$$

in which case the forward going high-energy stuff tends on average to decay well outside the nucleus radius, and to first order these fast particles do not depend upon the thickness of the nucleus. For the slow particles one expects a multiplicity roughly proportional to ν, the number of interactions in the nucleus. Equation 16 is not far from the simple mnemonic, $R \approx 1/2 + 1/2\bar{\nu}$, where the first term comes from that part of the multiplicity generated by the beam, while the second term would correspond to that coming from target fragmentation.

Actually the slow recoils from the target fragmentation region have a short enough formation length that some cascading in this region is possible. Such cascading can give particles in kinematic regions which would normally be forbidden in reactions off single nuclei. Numerous experiments have looked at slow backward protons, for example, and a whole class of theories has been developed to describe such interactions.[36] These theories go under various names such as coherent tube model, cumulative effect, and big hadron model. The physical picture in such models is different from that shown in Fig. 28; these

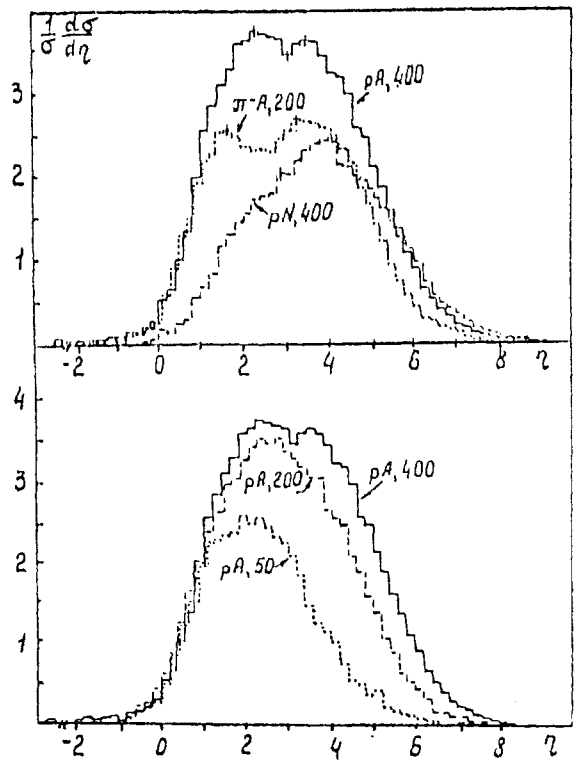

Fig. 30. Compilation of inclusive pseudorapidity distributions of fast ($\beta>0.7$) particles in emulsions compared with that off single nucleons, and also at the different incident laboratory momenta indicated in GeV (Boos *et al.* paper 307).

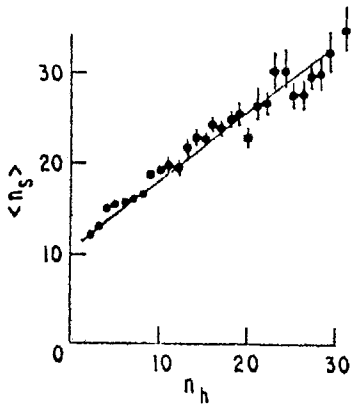

Fig. 31. Average multiplicity of fast particles from inelastic 400-GeV p-emulsion reactions as a function of the number of associated "heavy" tracks (Boos *et al.* paper 307).

models assume that the interaction takes place off ν nucleons which act together as a single coherent target and thus give a higher s value (by a factor of ν) than one would normally achieve with a hydrogen target.

Pseudorapidity distributions observed in emulsions are shown in Fig. 30. This compilation was taken from the very nice review paper of the Alma-Ata *et al.* collaboration (paper 307). While the target fragmentation region ($\eta<1$) depends strongly on A, it is independent of the beam identity and energy, as expected for limiting fragmentation. The dependence on A of the target extends well into the central region near $\eta=3$, a relatively long-range correlation between the target and central regions which is not expected in many models. In the beam fragmentation region there is a slight loss of particles as A increases. The central region grows and the curves move out in the beam fragmentation region as more phase space becomes available at higher energies. There is an indication of these distributions developing a double peak, one from the multiplication of slowish particles in the target fragmentation region, and the second from the usual peak near $x=0$.

One advantage of emulsion experiments is that they can count the number of heavily ionizing tracks, n_h, mainly recoil protons with $\beta<0.7$. As shown by Fig. 31, the average number of fast particles, $\langle n_s\rangle$, depends strongly on n_h, the data in the figure being well represented by the straight line

$$\langle n_s\rangle = 10.5 + 0.76\, n_h. \qquad (18)$$

The intercept of 10.5 is roughly 15% higher than the average value $\langle n_{\mathrm{chg}}\rangle=9$ found for pp reactions. The dependence of $\langle n_s\rangle$ on n_h can be compared with Eq. 16, suggesting that n_h is a measure of ν for a given event.

A relatively clean testing ground for ideas about reactions off nuclei is afforded by the deuterium nucleus, and many bubble chamber experiments have looked at such interactions. For example, a recent experiment[37] using a 360-GeV/c π^- beam found the double scattering probability to be (15 ± 2)% in deuterium. They further found the ratio of negatively charged particles produced in double scattering reactions to those from π^-p collisions to be $1.36\pm.07$, a value somewhat larger than, but consistent with, predictions based on AGK cutting rules or the coherent tube model.

A recent experiment on the A dependence of inclusive neutron production by 400-GeV protons has been carried out at Fermilab using a calorimeter to detect the forward-going neutrons. From their lead and beryllium data they obtain the values for a shown in Fig. 32, where $\sigma\propto A^{\alpha}$. As the neutron momentum increases above $x=0.15$, α falls

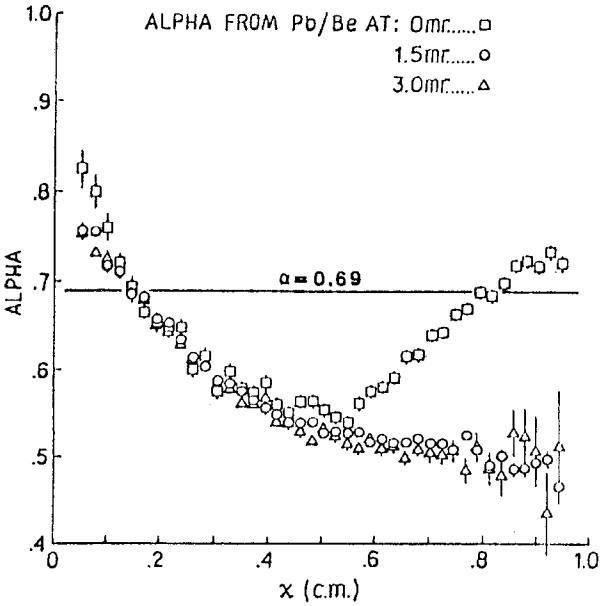

Fig. 32. Values of a calculated from lead/beryllium ratios of neutrons produced by 400-GeV protons (Whalley *et al.* paper 673).

below the value of 0.69 for the overall inelastic cross section, and fewer high-momentum neutrons are produced per interaction form lead than from beryllium. A similar effect is shown in Fig. 30 for fast charged particles in emulsions and has been observed in other counter experiments[38] as well. An exception to this trend is the 0-mrad neutron production shown in Fig. 32 where α increases again above $x=0.6$; this effect is not observed in the corresponding copper data, suggesting that the increase of fast neutrons off lead comes from coherent electromagnetic production processes (one-γ exchange) which would have a Z^2 dependence.

Another nuclear effect has been studied with an experiment[39] using $\pi^{\pm}$ beams on neon at 10 GeV; neglecting the production of $K^{\pm}$, $\bar{p}$ and assuming charge symmetry, one can estimate the momentum distribution of protons including those normally too fast to be identified in the usual way with ionization measurements. The average longitudinal momentum carried off by protons is shown in Fig. 33 as a function of the number of fast particles, n_s; for $n_s \geq 8$, the protons carry off on average ~ 2 GeV/c per event. Assuming an equal amount for the neutrons, this becomes a total of 4 GeV/c, a surprisingly large number considering that the experiment was carried out at only 10 GeV/c.

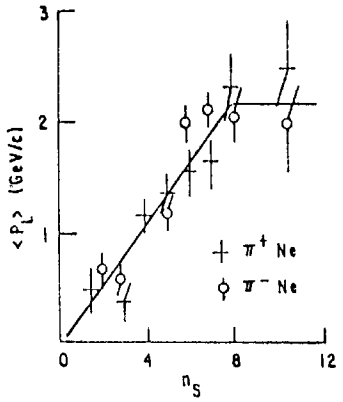

Fig. 33. Average laboratory longitudinal momentum per event carried off by protons produced in 10-GeV/c $\pi^{\pm}$ Neon collisions, as a function of the number of fast particles in the event (ref. 39).

A summary of some of the more important points concerning reactions off nuclei is as follows:

1. *Little cascading*—long time development.
2. Multiplicity *depends on* $\bar{\nu}$ rather than $A^{1/3}$; the hadronic state blasting it's way through the nucleus remembers the nature of the incident beam.
3. *KNO scaling approximately valid*, although $\langle n \rangle / D$ changes by $\sim 40\%$ depending on ν as measured by slow protons (n_h).
4. *Fast nucleons* often blasted out of nucleus; $\langle p_{\parallel} \rangle \sim 4$ GeV/c per event for $\pi^{\pm}$ Ne at 10 GeV and $n_s \geq 8$.
5. νA induced events much like πA: multiplicity distributions, fast protons, slow backward protons etc., are all very similar.[40]
6. *Many different models* can follow the data, but with little predictive power.

§12. Conclusions

1. The results of many experiments on multiplicities and correlations at different energies and with different beam particles have been presented to this Conference. With ever-increasing statistics, detailed effects such as three-body dynamic correlations can now be observed.
2. The compensation of charge and transverse momentum has been studied at the ISR with high statistics and has been used to discriminate between various cluster models.
3. Second order (Bose-Einstein) interference effects have been observed in several experiments and interpreted in terms of the

dimensions of the emission region. While this method holds promise for the study of the variation of these dimensions with different parameters, the variations thus far observed appear to come from differences in the treatment of the data.

4. Resonance production and decay appear to account for the majority of pions and kaons coming from high energy interactions, and analyses of inclusive distributions must take this into account if reliable results are to be obtained.

5. The ρ and A_2 trajectories have been obtained from a triple Regge analysis of pion charge exchange and η production, from both full-inclusive and neutrals-only final states; the results are in good qualitative agreement with those obtained from the energy dependence of the exclusive reactions.

6. Parton ideas, particularly as formulated by Das and Hwa, appear to be highly successful in describing the x distributions of leading nondiffractive particles at low p_T.

7. Charm production by hadron beams continues to be elusive; experiments with good signatures have thus far only been able to set upper limits, while more indirect experiments such as the SPS neutrino beam dump and the Fermilab single muon experiments observe signals which in some cases are larger than the previously quoted upper limits.

8. Emulsion experiments looking for short-lived charmed particles are also contradictory. Several experiments claim to have such events, but with different lifetimes and in violation of upper limits set by previous experiments.

9. My own guess is that inclusive charm production at Fermilab–SPS energies is of order 10 μb/nucleon with lifetimes of order 10^{-12} sec, but this will be resolved in the next year or two as much experimental effort is being devoted to the question.

10. The cosmic ray experiments continue to tantalize the rest of us who are tied to accelerator energies; they promise new types of strong interactions, Centauro events with high multiplicity but no π^0's, at the next generation of colliding-beam machines.

11. Interactions off nuclei are being actively pursued as a laboratory in which to study the space-time development of hadronic matter. The strong suppression of cascading inside nuclei is of fundamental importance and shows the relatively long evolution times involved.

Acknowledgments

In developing this talk I have greatly benefitted from innumerable discussions with many different people, both before and during this Conference, and I am grateful for their help. I would like also to thank my scientific secretary, Prof. T. Hirose, for his assistance in the preparation of the talk. The hospitality and efficient organization of our Japanese hosts have contributed greatly to the success of this Conference and is very much appreciated.

References

1. E. L. Berger: Nucl. Phys. **B85** (1975) 61.
2. M. LeBellac: Rapp. talk, Budapest Conf. (1977).
3. H. Kirk *et al.*: Nucl Phys. **B128** (1977) 397.
4. Irwin A. Pless: *IX Int. Sym. High Energy Multiparticle Dynamics* (Tabor, Czechoslovakia, July 1978).
5. C. Bromberg *et al.*: Phys. Rev. Letters **38** (1977) 1447.
6. G. Kopylov and M. Podgoretsky: Sov. J. Nucl. Phys. **18** (1973) 656; **19** (1974) 434; G. Cocconi: Phys. Letters **49B** (1974) 459.
7. M. Deutschmann *et al.*: CERN/EP/PHYS 78–1 (Jan. 1978).
8. The K^+p data at 32.1 GeV/c are from M. Goossens *et al.*, paper 444; the pp data from the ISR are from D. Drijard *et al.*, paper 273; and the $\bar{p}p \to K_s K_s X$ data at 0.76 GeV/c are from A. M. Cooper *et al.*, Nucl. Phys. **B139** (1978) 45. The other points are taken from the compilations presented in the aobve papers.
9. H. Grässler *et al.*: Nucl. Phys. **B132** (1978) 1.
10. D. Cutts *et al.*: Phys. Rev. Letters **40** (1978) 141.
11. H. Kirk *et al.*: Nucl. Phys. **B128** (1977) 397.
12. A. V. Barnes *et al.*: Caltech preprint CALT–68–667 (June 1978).
13. A. V. Barnes *et al.*: Phys. Rev. Letters **37** (1976) 76; O. I. Dahl *et al.*: Phys. Rev. Letetrs **37** (1976) 80.
14. B. Andersson: Phys. Letters **69B** (1977) 221.
15. Hyman Goldberg: Nucl. Phys. **B44** (1972) 149; S. Pokorski and L. Van Hove: Acta Phys. Pol. **B5** (1974) 229; Nucl. Phys. **B86** (1975) 243; and CERN preprint TH. 2427 (Nov. 1977).
16. Wolfgang Ochs: Nucl. Phys. **B118** (1977) 397.
17. K. P. Das and R. C. Hwa: Phys. Letters **68B** (1977) 459.
18. D. W. Duke and F. E. Taylor: Phys. Rev. **D17** (1978) 1788.
19. L. Lederman: rapporteur talk at this Conference.
20. F. C. Erné and J. C. Sens: CERN preprint (Jan. 1978).
21. J. Singh *et al.*: Nucl. Phys. **B140** (1978) 189.

22. W. Lockman *et al.*: Phys. Rev. Letters **41** (1978) 680.
23. T. A. DeGrand and H. I. Miettinen: Phys. Rev. Letters **40** (1978) 612.
24. S. J. Brodsky and J. F. Gunion: Phys. Rev. **D17** (1978) 848.
25. Data used for Fig. 21 come from a) D. Cutts *et al.*, paper 413 (100, 175 GeV/*c*); b) M. Barth *et al.*, paper 338 (70 GeV/*c*); c) R. T. Edwards *et al.*, Phys. Rev. **D18** (1978) 76 (200 GeV/*c*); d) K. Böckmann, Talk at the Symposium on Hadron Structure and Multiparticle Production, Kazimierz (1977) (16 to 225 GeV/*c*); e) ref. 22 ($\sqrt{s}$ =53 GeV).
26. R. N. Cahn: Phys. Rev. Letters **40** (1978) 80.
27. Yu. M. Antipov *et al.*: papers 204 and 941; K.-F. Albrecht *et al.*: paper 149; A. M. Jonckheere *et al.*: Phys. Rev. **D16** (1977) 2073 and H. Lubatti: private communication; M. A. Abolins *et al.*: Phys. Rev. Letters **37** (1976) 417; D. Spelbring: Pphys. Rev. Letters **40** (1978) 605; R. Lipton *et al.*: Phys. Rev. Letters **40** (1978) 608; M. J. Lauterbach: Phys. Rev. **D17** (1978) 2507; W. R. Ditzler: Phys. Letters **71B** (1977) 451; L. Baum: Phys. Letters **77B** (1978) 337; A. G. Clark: Phys. Letters **77B** (1978) 339; K. W. Brown: paper 1011; A. Soukas *et al.*: paper 1156; A. E. Asratyan: paper 288; T. Hansl *et al.*: Phys. Letters **74B** (1978) 139; P. Alibran *et al.*: Phys. Letters **74B** (1978) 134; P. C. Bosetti *et al.*: Phys. Letters **74B** (1978) 143. For a review of the CERN beam dump experiments see also H. Wachsmuch, talk at the Oxford Neutrino Conf. (July 1978).
28. Particle Data Group: Phys. Letters **75B**, No. 1 (Apr. 1978).
29. J. H. Cobb *et al.*: Phys. Letters **73B** (1978) 497.
30. T. K. Gaisser and F. Halzen: Phys. Rev. **D14** (1976) 3153.
31. C. Quigg: Fermilab preprint Conf.-78/37–THY (Aprl: 1978) and minirapporteur talk in Session B8.
32. D. J. Crennell *et al.*: Rutherford preprint RL–78–051 A (June, 1978).
33. F. Halzen and S. Matsuda: Phys. Rev. **D17** (1978) 1344.
34. Private communication from E. L. Berger and T. Kamae.
35. J. E. Elias *et al.*: Phys. Rev. Letters **41** (1978) 285.
36. For a comparative review of various models describing high energy interactions in nuclei see B. Andersson: *Proc. Int. Colloq. on Multiparticle Reactions* (Tutzing, 1976 p. 109.
37. K. Moriyasu *et al.*: Nucl. Phys. **B137** (1978) 377.
38. K. Heller *et al.*: Phys. Rev. **D16** (1977) 2737; D. Chaney *et al.*: Phys. Rev. Letters **40** (1978) 71; however, the neutron induced data of D. L. Burke *et al.*: paper 676, show little change in the yield per inelastic collision of particles with pseudorapidity $\gtrsim 5.5$.
39. W. M. Yeager *et al.*: Phys. Rev. **D16** (1977) 1294.
40. T. H. Burnett *et al.*: U. of Wash. preprint VTL–PUB–55 (1977) and H. Lubatti: private communication; J. P. Berge *et al.*: Fermilab Pub.-78/55 (1978).

P2a: Large P_T Phenomena, Jet Structure

Chairman: G. VON DARDEL
Speaker: R. SOSNOWSKI
Scientific Secretaries: K. NAKAMURA
T. INAGAKI

P2b: Prompt Dilepton Production by Hadron Reaction

Chairman: P. FALK-VAIRANT
Speaker: L. LEDERMAN
Scientific Secretaries: M. MISHINA
A. MAKI

(Monday, August 28, 1978; 11: 30–12: 30, 14: 00–15: 00)